Selectively modifying the interaction of human Tuba SH3-6 domain with listerial InlC and human N-WASP

By

Kofi Kwantwi Boafoh

Student number: 13136730

UNIVERSITEIT VAN PRETORIA
UNIVERSITY OF PRETORIA
YUNIBESITHI YA PRETORIA

Dissertation submitted in partial fulfilment for the degree *Magister Scientiae* (MSc) at the Department of Biochemistry, Genetics and Microbiology, Natural and Agricultural Sciences Faculty, University of Pretoria

Supervisor: Prof Wolf-Dieter Schubert

DECLARATION OF ORIGINALITY UNIVERSITY OF PRETORIA

The Department of Biochemistry, Genetics and Microbiology places great emphasis upon integrity and ethical conduct in the preparation of all written work submitted for academic evaluation. While academic staff teach you about referencing techniques and how to avoid plagiarism, you too have a responsibility in this regard. If you are at any stage uncertain as to what is required, you should speak to your lecturer before any written work is submitted.

You are guilty of plagiarism if you copy something from another author's work (e. g a book, an article or a website) without acknowledging the source and pass it off as your own. In effect you are stealing something that belongs to someone else. This is not only the case when you copy work word-for-word (verbatim), but also when you submit someone else's work in a slightly altered form (paraphrase) or use a line of argument without acknowledging it. You are not allowed to use work previously produced by another student. You are also not allowed to let anybody copy your work with the intention of passing if off as his/her work. Students who commit plagiarism will not be given any credit for plagiarized work. The matter may also be referred to the Disciplinary Committee (Students) for a ruling. Plagiarism is regarded as a serious contravention of the University's rules and can lead to expulsion from the University. The declaration which follows must accompany all written work submitted while you are a student of the Department of Biochemistry. No written work will be accepted unless the declaration has been completed and attached.

Full names of student: Kofi Kwantwi Boafoh
Student number: 13136730
Topic of work: Selectively modifying the interaction of human Tuba SH3-6 domain with listerial InlC and human N-WASP

1. I understand what plagiarism is and am aware of the University's policy in this regard.

2. I declare that this dissertation is my own original work. Where other people's work has been used (either from a printed source, Internet or any other source), this has been properly acknowledged and referenced in accordance with departmental requirements.

3. I have not used work previously produced by another student or any other person to hand in as my own.

4. I have not allowed, and will not allow, anyone to copy my work with the intention of passing it off as his or her own work.

SIGNATURE:  **DATE**: MARCH 2020

Acknowledgements

First and foremost, I would like to thank GOD for HIS protection and guidance throughout my studies.

I would also like to express my sincere gratitude to the following people:

- My parents (Joseph Alexander Boafoh, and Augustina Nsiah Boafoh) and my siblings (Akwasi Boafo Barima, and Edin Dwuma Boafo) who have been very supportive throughout my educational journey. Without their support and encouragement, possibly I would not have reached this far in life. I really appreciate their contribution in my life.

- My supervisor, Professor Wolf-Dieter Schubert for giving me the opportunity to undertake this project. Thank you for the contributions you made towards my project. It was a privilege to be in the Structural Biology research group as I have learnt a lot in this field.

- Dr Precious Motshwene for his constructive questions and suggestions towards my project.

- Dr Ben Mans for assisting me with my isothermal titration calorimetry experiments.

- Last but not the least, thanks to present and past colleagues (Mr Mthwelanga Ndengane, Mr Ade Adewumi, Mr Clifford Ntui, Ms Erna Freyer, Ms Marissa Poolman, Ms Lenye Dlamini, Mr Hildsley Noome, Mr Eugene Duvenage, Ms Siphokazi Ncwaiba, Ms Clare Boswell) from the Structural Biology of Infectious Disease research group, University of Pretoria. Their criticisms, opinions and suggestions during our research group meetings contributed towards my completion of this project.

- Special thanks to the National Research Foundation (NRF) for awarding me the NRF Free-standing Master's Scholarship for the duration (2017-2019) of my studies.

Summary

Listeriosis is a food-borne disease caused by the gram-positive bacterium *Listeria monocytogenes*. In extreme cases, listeriosis can lead to sepsis and meningitis. The bacterium uses host actin cytoskeleton for its own motility and to deform the cell membrane and create protrusions into neighbouring cells. Cell-to-cell spread is a hallmark of listeriosis, and it is linked to the virulence protein InlC. InlC binds the sixth SH3 domain of human Tuba (SH3-6), an actin-organising protein and in doing so displaces N-WASP, the main physiological binding partner of Tuba SH3-6. InlC thereby enables listerial protrusion formation and cell-to-cell spread. However, knocking out InlC reduces protrusion formation by only 50 %. To help resolve which other listerial or host factors promote protrusion formation and cell-to-cell spread, this study aims to decouple the interdependence of InlC and N-WASP binding to Tuba SH3-6.

Crystal structures of the Tuba SH3-6 / N-WASP and Tuba SH3-6 / InlC complexes, were analysed and suitable modifications of Tuba SH3-6 were chosen to weaken the interaction of one partner to Tuba SH3-6 without affecting the other. Mutant plasmids of Tuba SH3-6 were generated by site-directed mutagenesis and variant proteins produced and purified chromatographically. Binding affinities between Tuba SH3-6 variants and either InlC or N-WASP were quantified by isothermal titration calorimetry, using the interaction of wild-type proteins as control experiments and to establish the congruency with previous studies. Variants of Tuba SH3-6 with reduced affinity for either InlC or N-WASP were used in co-crystallization experiments with the other partner to confirm the mode of binding.

Binding of InlC to wild-type Tuba SH3-6 and InlC yielded a K_D value in agreement with published data. However, N-WASP titration into wild-type Tuba SH3-6, as well as Tuba variants N1535A, Y1570A or W1554A, invariably yielded a dissolution of an N-WASP dimer or higher oligomer presumably induced by the high N-WASP peptide concentrations required to quantify weak binding. Similar non-sigmoidal curves were observed for reactions of InlC with Tuba SH3-6 variants Y1570A or W1554A. This was again interpreted as the probable dissolution of possible concentration-induced InlC dimer masking complex formations. Overall, only variant Tuba E1575A had an impact on interaction with its binding partner. The variant E1575A yielded a weaker and stronger interaction with InlC and N-WASP, respectively. This variant will be useful in an *in vivo study* to further investigate the underlying factors involved in cell-to-cell spread. The wild-type InlC crystal structure solved with an improved resolution at 1.85 Å relative to 2.05 Å of a previous study, will be deposited onto the protein data bank.

Key words: *Listeria monocytogenes,* InlC, N-WASP, Tuba SH3-6, cell-to-cell spread, ITC, crystallization

Table of Contents

List of Figures

List of Tables

Abbreviations

ActA	Actin assembly-inducing protein
BAR	Bin-amphysin-Rvs (domain)
c-Met	Mesenchymal epithelial transition factor (MET)
DH	Dbl homology (domain)
dNTP	deoxyribonucleotide triphosphate
E. coli	*Escherichia coli*
Ecad	E-cadherin
ERM family protein	Ezrin, radixin and moesin
F-actin	Filamentous actin
GC	Guanine + Cytosine (content of DNA)
G-actin	Globular actin
GS	Glutathione sepharose
His_6	Six histidine
HRV-3C protease	Human rhinovirus 3C protease
Ig	Immunoglobulin
InlA	Internalin
IPTG	Isopropyl β-D-1 thiogalactopyranoside
IR	Inter-repeat
ITC	Isothermal titration calorimetry
LLO	Listeriolysin
Lm	*Listeria monocytogenes* (*L. monocytogenes*)
LLR	Leucine-rich repeat
NPF	Nucleation-promoting factor
N-WASP	Neuronal Wiskott-Aldrich Syndrome Protein
PBS	Phosphate buffered saline
PCR	Polymerase chain reaction
PDB	Protein data bank
p.i.	post infection
RT	Room temperature
SDM	Site-directed mutagenesis
SH3	Src Homology 3 (domain)
SH3-6	Sixth Src Homology 3 domain of Tuba
SrtA	Sortase A
TB	Transformation buffer
WT	Wild-type

1 Introduction

Bacterial pathogens are a major cause of water and food-borne mammalian diseases resulting in an estimated 2.2 million human deaths per annum from gastroenteritis alone (Kuchenmüller *et al.*, 2013). A few of these bacteria are entero-invasive pathogens, characterised by their ability to induce their own uptake by non-phagocytic intestinal epithelial cells (Cossart and Sansonetti, 2004). Once inside a cell, these bacteria replicate, subvert the immune system and continue to colonise the host by spreading from cell-to-cell and to different organs via the blood stream (Cossart and Toledo-Arana, 2008). Bacteria of this category include *Yersinia*, *Shigella*, *Salmonella* (Reis and Horn, 2010) and *Listeria monocytogenes* (*L. monocytogenes* or *Lm)* (Barbuddhe and Chakraborty, 2009). Amongst entero-invasive bacteria, *L. monocytogenes* has immerged as a model organism owing to its relatively low pathogenicity, ease of culturing, and high loads of infections in laboratory mice (Pamer, 2004).

1.1 Listeria monocytogenes

In addition to *L. monocytogenes*, the genus *Listeria* contains the species *L. rocourtiae*, *L. marthii, L. seeligeri*, *L. ivanovii*, *L. innocua*, *L. welshimeri and L. grayi* in (Graves *et al.*, 2010). Most are non-pathogenic except *L. ivanovii*, which infects animals, and *L. monocytogenes*, which infects both animals and humans (Furrer *et al.*, 1991, Orsi *et al.*, 2011). As a member of the Firmicutes phylum, *Lm* is a gram-positive bacterium with a high genetic AT content (Buchrieser, 2007). Normally, *Lm* is a motile saprophyte, living on decaying plant material (Gray and Killinger, 1966). The bacterium survives and multiplies in extreme conditions such as near freezing temperatures (Pöntinen *et al.*, 2015), acidic and high salt concentrations - conditions that are used in food processing and preservation (Vázquez-Boland *et al.*, 2001). The latter partly explain the success of this food-borne pathogen (Allerberger and Wagner, 2010).

Listeriosis is a rare but potentially fatal foodborne infection caused by the bacterium *Lm.* Humans who ingest *Lm*-contaminated food mostly develop non-invasive listeriosis resulting in febrile gastroenteritis. Immunocompromised individuals, by contrast, experience invasive listeriosis characterized by bacteraemia, septicaemia, meningitis and meningoencephalitis (Aureli *et al.*, 2000). Immunocompromised individuals such as the aged, foetuses and pregnant

women are vulnerable to listeriosis (Schlech III and Acheson, 2000) with a 12-fold higher risk for pregnant women compared to the average population (Hof, 2003).

The annual incidence of invasive listeriosis is estimated to be about 4 cases in 1 000 000 people in the United States and Europe (Pöntinen *et al.*, 2015, Goulet *et al.*, 2011). Although reported incidences of listeriosis are low, the mortality rate of 20 to 30 % of confirmed infections makes it the most serious among foodborne diseases (Newell *et al.*, 2010). The largest listeriosis outbreak internationally was witnessed in South Africa between January 2017 and March 2018. The outbreak affected more than 674 patients of whom 183 (27 %) were killed by the disease. Correspondingly, 42 % of infections in the 2017/2018 outbreak affected neonates (WHO, 2018).

1.2 Pathophysiology of listeriosis

The incubation period for listeriosis varies depending on host immunity. Febrile gastroenteritis normally occurs within 24 h post infection (p.i.), bacteraemia within two days, central nervous system infections within nine days and pregnancy associated listeriosis up to 67 days p.i. (Goulet *et al.*, 2013). These periods correspond to dissemination rates to various host organs (Figure 1.1) reflecting the fact that this requires the bacterium to cross tight physiological barriers such as the intestinal, the blood-brain and the foetoplacental barriers (Camejo *et al.*, 2011). *Lm* crosses the intestinal barrier by transcytosis (Nikitas *et al.*, 2011) and disseminates from mesenteric lymph nodes and bloodstream to the liver and the spleen (Lecuit, 2007, Camejo *et al.*, 2011). The liver clears most listeria from the circulatory system. Surviving bacteria, however, replicate within splenic and hepatic macrophages, hepatocytes or epithelial cells. Resulting cell lysis re-introduces bacteria into the bloodstream to cross the blood-brain barrier and the foetoplacental barrier causing potentially fatal brain and placental infections (Camejo *et al.*, 2011).

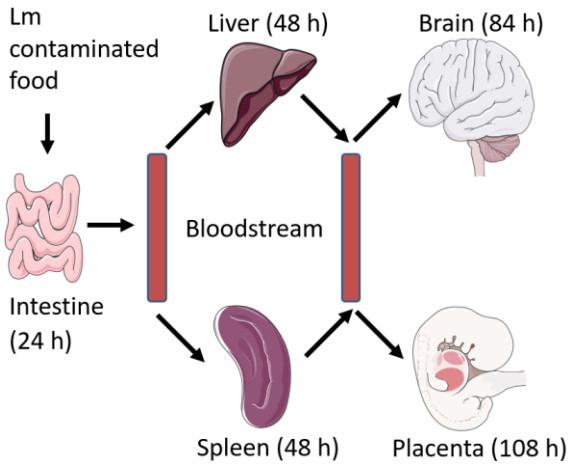

Figure 1.1: ***L. monocytogenes* dissemination routes inside a mammalian host.**

After ingesting contaminated food, *L. monocytogenes* colonises the gastrointestinal tract within 24 h, reaches the lymph nodes in 36 h, and spreads to the liver and spleen *via* the bloodstream within 48 h p.i. It crosses the blood-brain barrier after 84 h and the placental barrier after 108 h to infect unborn foetuses. Adapted from Lecuit, 2007.

1.3 Cellular infection cycle of *L. monocytogenes*

As part of its infection mechanism, *Lm* invades, survives and replicates within non-phagocytic cells, such as epithelial cells and hepatocytes (Figure 1.2).

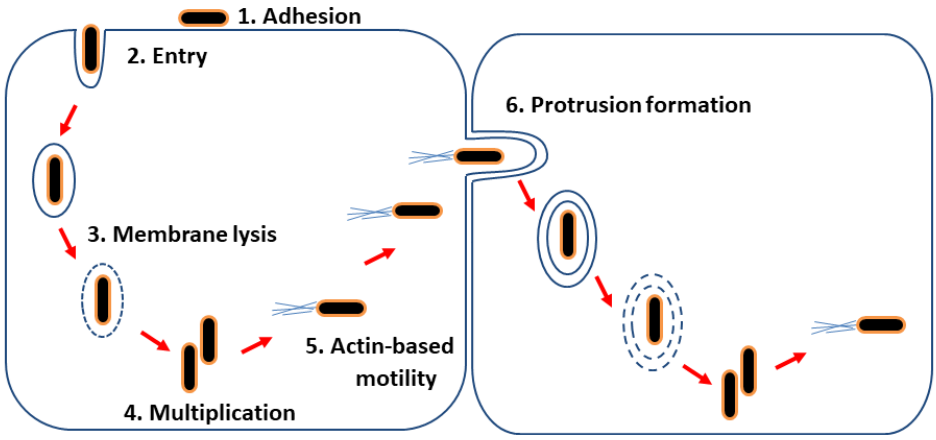

Figure 1.2: **Cellular infection cycle of *L. monocytogenes* in mammalian target cells.**

1) *Lm* recognizes and binds to intestinal epithelial cells through the virulence factors InlA and InlB that respectively interact with E-cadherin and hepatocyte growth factor receptor c-Met. **2)** Following adhesion, both

InlA and InlB signal through their receptors inducing phagocytosis by the host cell. **3)** Following engulfment, *Lm* secretes listeriolysin and two phospholipases C to lyse the phagosome. **4)** *Lm* escapes into the cytosol and replicates. **5)** The bacterium presents ActA near one of its poles to polymerize the actin cytoskeleton providing a force for bacterial motility. **6)** Upon encountering the cell membrane, *Lm* can locally weaken the cortical actin cytoskeleton by the secretion of InlC resulting in membrane protrusions into neighbouring cells. Following engulfment by the neighbouring cell, the bacterium infects new cell and continues the infection cycle. Adapted from Pizarro-Cerdá and Cossart, 2006.

The cellular infection cycle of *Lm*, as detailed in Figure 1.2, involves the steps: **1)** adhesion, **2)** invasion, **3)** escape, **4)** multiplication, **5)** actin-based motility and **6)** protrusion formation.
1) Adhesion, the bacterium attaches itself and engages with specific host cell receptors InlA characterized by a sorting signal at the carboxyl-terminal, which is used in covalent attachment to bacterial cell wall (Bierne *et al.*, 2002, Cabanes *et al.*, 2002). **2)** The interactions of InlA and InlB respectively with E-cadherin (Ecad) and hepatocyte growth factor receptor c-Met, respectively trigger signalling cascades, resulting in actin polymerization, which causes the host membrane to surround and engulf bacterium (Pizarro-Cerdá and Cossart, 2006) called a "zippering" mechanism in *Lm* (Lecuit *et al.*, 1997, Mengaud *et al.*, 1996). **3)** After invasion, the engulfed bacterium is in a phagosome. It secretes cholesterol-dependent listeriolysin (LLO) (Mengaud *et al.*, 1988) to create pores of different sizes(Jacobs *et al.*, 1998). Apart from lysing the bacterial vacuole, LLO increases the likelihood of the initial invasion step (Pizarro-Cerdá and Cossart, 2006). LLO also acts together with two secreted phospholipases C (PlcA and PlcB) to create pores by cleaving the polar heads of phospholipids at the glycerol-to-phosphorus bond (Smith *et al.*, 1995). **4)** Following bacterial escape, it grows and multiplies in the cytoplasm (Schnupf and Portnoy, 2007). **5)** By presenting the virulence protein actin assembly-inducing protein (ActA), which actively coordinates the production of new actin filaments adjacent to the cell wall (Lecuit, 2005). ActA mimics the nucleation-promoting factor Wiskott-Aldrich syndrome protein (WASP) that contains both actin-binding and acidic regions to activate the actin-related protein 2/3 complex (Welch *et al.*, 1998). Thus ActA polymerizes actin to create a comet-like tail (Ireton, 2013) resulting in random motility within the host cell (Kocks *et al.*, 1992). By *Lm* motility, ActA also allows the bacterium to escape autophagy (Travier *et al.*, 2013). **6)** Rapid

moving bacteria make contact to host plasma membrane. Upon encountering, *Lm* secretes InlC, which displaces N-WASP from the host Tuba SH3-6, locally weakening the cortical tension to create protrusions. The formed protrusions are engulfed by neighbouring cells causing bacterium enclosure into another vacuole and the infection cycle continues again (Lecuit, 2005).

1.4 InlC

PrfA-regulated gene, *inlC* was discovered in the genomes of *L. monocytogenes* and *L. ivanovii* but absent in non-pathogenic *Listeria* (Engelbrecht *et al.*, 1996). InlC is a secreted virulence factor. In listerial cultures, InlC is found in the supernatant following secretion but is absent from cell wall surface. This finding correlates with the presence of the N-terminal secretion signal sequence of InlC, with no cell wall anchor domain at the C-terminal (Bierne and Cossart, 2007). InlC was found to be related to both InlA and InlB (Engelbrecht *et al.*, 1996), later found to be a member of the internalin protein family. Internalins are characterized by leucine-rich repeats (LRR) domain, sandwiched between N-terminal short cap and C-terminal inter-repeat (IR) domain (Schubert *et al.*, 2001, Bierne and Cossart, 2007). The LRR domain is often implicated in protein-protein interactions. Intracellular expression and InlC possession of LRR domain, suggest that InlC regulates protrusion formation.

Work done by Rajabian *et al.,* 2009 identified InlC to play a role in listerial protrusion formation by engaging with human scaffolding protein Tuba. Protrusion formation was quantified by assessing the bacterial comet tails that possess ezrin. Ezrin from the ERM family protein is used as a marker for protrusions because comet tails in protrusions contain ezrin but those in the cell body lack it. In comparing a wild-type listeria strain, a mutant with deleted *inlC* had 43 % decrease of comet-like tails possessing ezrin. Thus, protrusion formation was compromised since the mutant was less efficient to produce comet-like tails (Rajabian *et al.*, 2009).

1.5 Tuba SH3-6 in listerial protrusion formation

The scaffolding protein, human Tuba consists of multiple domains that connects cytoskeletal dynamics and membrane trafficking pathways (Kovacs *et al.*, 2006). Figure 1.3 a) below depicts the human Tuba, which is a 180 kDa protein consisting of various functional domains including six Src Homology 3 (SH3) domains, a Dbl homology (DH) domain and a lipid-binding Bin-amphysin-Rvs (BAR) domain (Salazar *et al.*, 2003). The first four N-terminal SH3 domains are binding sites for human dynamin, whereas no ligand has been identified to bind the fifth SH3 (SH3-5) domain. The C-terminus contains domains that can interact with signalling pathways and cytoskeletal regulatory elements. Most of these SH3 domains interact with proline-rich (PxxP) sequences. As shown in Figure 1.3 b), N-WASP binds the SH3-6 domain. This interaction controls the morphology and tight cellular junctions between cells (Bierne and Cossart, 2007). However, in listerial infection, intracellular *Lm* secretes InlC, which binds to Tuba SH3-6 to displace its physiological partner, N-WASP as shown in Figure 1.3 c). This diminishes the cortical actin tension and weakens the junctional membrane permitting protrusion formations by motile bacteria (Otani *et al.*, 2006, Leung *et al.*, 2013).

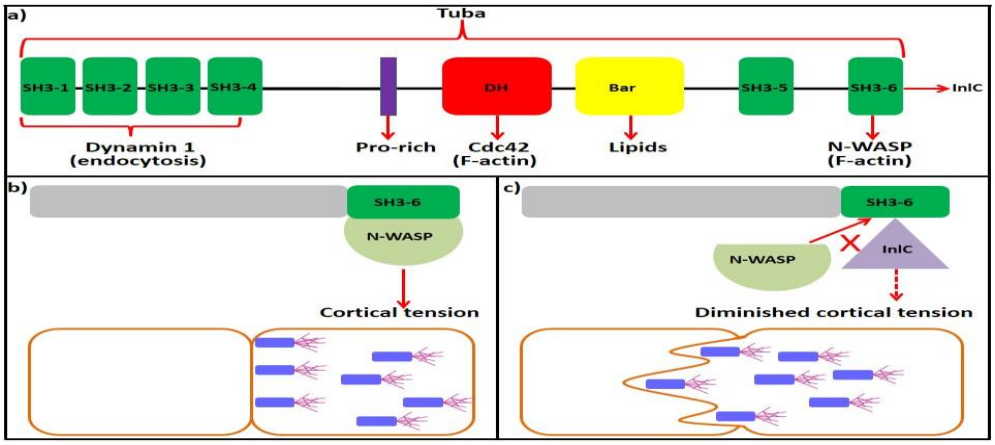

Figure 1.3: **Protein interactions and their effect on the cell**.

a) The scaffolding protein, human Tuba consisting of functional domains b) Proline-rich N-WASP binds the SH3-6 to promote cortical tension formation, which maintains cell integrity (Salazar *et al.*, 2003). c) The virulence factor InlC triggers cell-to-cell spread of *Lm* by binding to the sixth SH3 domain (SH3-6) and displacing its physiological partner N-WASP. This diminishes the cortical actin tension and weakens the junctional membrane for motile bacteria to form protrusions. Adapted from Ireton *et al.*, 2014.

1.6 Project rationale

The virulence factor InlC triggers cell-to-cell spread by binding to the Tuba SH3-6 and displacing its physiological partner N-WASP. Listerial virulence is critically dependant on this type of cell-to-cell spread (Rajabian *et al.*, 2009, Leung *et al.*, 2013). However, knocking out InlC reduces protrusion formation and cell-to-cell spread by 50 %, but it does not disappear (Rajabian et al., 2009, Polle *et al.*, 2014). It remains unclear whether other listerial factors also promote protrusion formation and cell-to-cell spread Hence, this study aims to help us further understand how these processes work.

Crystal structures of Tuba SH3-6 / InlC and Tuba SH3-6 / N-WASP complexes reveal that surface regions of these complexes partly overlap. However, there are also unique regions through which Tuba SH3-6 only interacts with one of its binding partners (InlC or N-WASP) (Polle *et al.*, 2014). To investigate whether Tuba SH3-6 accounts for the other factor of protrusion and cell-to-cell spread process, these regions whereby Tuba SH3-6 exclusively binds to either InlC or N-WASP will be analysed to identify critical amino acids for mutations. Mutant plasmids of Tuba SH3-6 will be generated by site-directed mutagenesis while variant proteins will be produced and purified chromatographically. Furthermore, protein interaction studies by isothermal titration calorimetry (ITC) will provide insight and molecular tool for biologists to further study *L. monocytogenes* cell-to-cell spread *in vivo*.

1.7 Hypothesis, Aim and Objectives

1.7.1 Hypothesis

It will be possible to selectively manipulate the interaction of Tuba SH3-6 with either one of its interaction partners N-WASP or listerial InlC by substituting critical residues of Tuba SH3-6 by alanine.

1.7.2 Aim

Develop variants of Tuba SH3-6 retaining affinity for either InlC or N-WASP but not the other for downstream analysis of cell-to-cell spread.

1.7.3 Objectives

- Analyse available structures of the InlC / Tuba SH3-6 and Tuba SH3-6 / N-WASP protein complexes to identify suitable amino acid substitutions in human Tuba SH3-6 that would weaken its interaction with either InlC or N-WASP – ideally without affecting the other.
- Substitute residues of Tuba SH3-6 identified above by site-directed mutagenesis (SDM) and confirm the mutations at the DNA level by Sanger sequencing.
- Produce and purify InlC as well as variants and wild-type Tuba SH3-6.
- Determine binding affinities of Tuba SH3-6 variants with both InlC and N-WASP by isothermal titration calorimetry (ITC) to establish the degree to which proposed mutations affect interaction with individual binding partner.
- Crystalize and structurally analyse complexes of Tuba SH3-6 variants with either InlC or N-WASP to confirm the mode of binding.

2 Materials and Methods

2.1 Identifying Tuba SH3-6 Mutations

The listerial virulence factor InlC binds Tuba SH3-6 to prevent its physiological complex with N-WASP, diminishing the host cortical actin tension and subsequently leading to cell-to-cell spread. The crystal structure of Tuba SH3-6 in complex with both its physiological binding partner N-WASP and listerial InlC have been solved previously providing a wealth of data on the molecular recognition such as hydrogen bonds or Van der Waals interactions. These complexes were superimposed and analysed in three-dimensional space to identify residues in Tuba SH3-6 that are critical to the complex formation with only the one binding partner or the other. These residues were to be replaced by alanine to remove its contribution to the interaction and thereby weaken the molecular interaction. Table 2.1 below summarizes the residues identified in this process and the proposed effect that substitution by alanine would have on the protein-protein interaction.

Table 2.1: Tuba SH3-6 residue substitutions with alanine

Original residue	Substituted residue	Expected impact
Asn1535	Ala1535	Weaken N-WASP / Tuba SH3-6 interaction, without affecting InlC / Tuba SH3-6 interaction
Glu1575	Ala1575	
Tyr1570	Ala1570	Weaken InlC / Tuba SH3-6 interaction, without affecting N-WASP / Tuba SH3-6 interaction
Trp1554	Ala1554	

2.2 Materials and equipment

Experiments were conducted using materials and equipment at the University of Pretoria main campus in the Department of Biochemistry, Genetics and Microbiology. Isothermal titration calorimetry experiments were conducted at the Onderstepoort Veterinary Institute, Department of Biochemistry.

Table 2.2: List of equipment

Equipment	**Model name**	**Manufacturer**
Centrifuges	5417C	Eppendorf (Hamburg, Germany)
	Heraeus Megafuge 8R	Thermo Fisher Scientific (Massachusetts, USA)
	Sorvall Lynx 6000	
Concentrator	Amicon Ultra 15 mL centrifugal filters	Merck (Darmstadt, Germany)
Cell Density Meter	CO 8000	Biochrom (Cambridge, UK)
Chromatography columns	10 mL drip column with 35 µm filter pore size	MoBiTech (Goettingen, Germany)
	ENrich SEC 70 10/300	Bio-Rad (Hercules, CA, USA)
Incubator	Multitron	Infors (Bottmingen, Switzerland)
Gel imager	Molecular Imager GelDoc XR and UV transilluminator	Bio-Rad (Hercules, CA, USA)
Polyacrylamide gel electrophoresis chamber	Mini-PROTEAN	
Electrophoresis power pack	Power Pac Basic	
PCR thermocycler	T100 Thermocycler	
Microscopes	Keyence Leica DFC320	Keyence (Osaka, Japan)
	Zeiss Discovery V8	Zeiss (Oberkochen, Germany)
Microcalorimeter	MicroCal ITC200	GE Healthcare (Illinois, USA)

Nanodrop	ND-100 Spectrophotometer	Thermo Fisher Scientific (Massachusetts, USA)
pH meter	320 pH Meter	Mettler Toledo (California, USA)
Roller	Roller Mixer SRT6	Stuart Scientific (Staffordshire, UK)
Sonicator	Q500	QSonica (Connecticut, USA)

2.3 Reagents and chemicals

Reagents and chemicals used were purchased from suppliers. Table 2.3 shows a list of reagents and chemicals with their corresponding suppliers.

Table 2.3: List of reagents and chemicals

Reagents	**Supplier**
Phusion Hot Start II DNA polymerase	Thermo Fisher Scientific (Massachusetts, USA)
Ammonium persulphate (APS), Agar, HCl, NaCl, Na acetate, SDS, Tris, Tryptone, Yeast extract	Merck (Darmstadt, Germany)
Ampicillin	Separations (Johannesburg, South Africa)
Deoxynucleotides	Merck (Darmstadt, Germany)
DpnI	New England Biolabs (Massachusetts, USA)
Dithiothreitol (DTT)	Roche (Basel, Switzerland)
GeneJet Plasmid Miniprep kit, tetramethylenediamine (TEMED)	Thermo Fisher Scientific (Massachusetts, USA)
Isopropyl β-D-1 thiogalactopyranoside (IPTG), Sequencing primers (forward and reverse)	Inqaba biotech (Pretoria, South Africa)
N-WASP peptide	Helmholtz Centre for Infection Research (Braunschweig, Germany)
Precision plus protein marker (10-250 kDa)	Bio-Rad (California, United States)

2.4 Stock solutions, buffers, and growth media

Stock solutions and buffers prepared were filtered (0.2 µm filter) and degassed using a vacuum blotting pump. For sterilization, filtered solutions and growth media were autoclaved at 121 °C for 20 min. Solutions and buffers were adjusted by adding drops of either 1M HCl or 1M NaOH until the desired pH was reached.

Table 2.4: Reagents prepared for general protein production

Description	Purpose	Preparation
Ampicillin stock solution (100 mg/mL)	Antibiotic	1 g ampicillin was dissolved in 10 mL distilled water (dH_2O) and filter sterilized through 0.22 µm filter. Aliquots of 1 mL were kept at -20 °C.
IPTG stock solution	Induction of gene expression	1 mL aliquots of 0.1 mM IPTG stock solution were kept at -20 °C.
Lysogeny broth (LB)	*E. coli* propagation	10 g tryptone, 5 g yeast and 5 g NaCl were dissolved in 1 L dH_2O and autoclaved.
LB agar plates	Solid growth medium	15 g agar was added in 1 L LB and sterilized by autoclaving. It was cooled at room temperature (RT) and 2 µL of 50 mg/mL ampicillin stock solution was added to achieve a final working concentration of 100 µg/mL ampicillin. The sterilized LB agar was poured into petri-dishes and stored at 4 °C.

Table 2.5: List of general solutions and buffers

Description	Purpose	Content
5 x Sequencing buffer	Sanger sequencing	From Thermo Fisher Scientific; kept at -20 °C.
5 M Sodium acetate buffer	Ethanol precipitation	40.8 g of NaOAc dissolved in 100 mL dH_2O. Aliquots of 1 mL were kept at -20 °C.
10 x Phosphate buffered saline (PBS)	Buffer	80 g NaCl, 2 g KCl, 14.4 g $NaHPO_4.2H_2O$ and 4.8 g KH_2PO_4 dissolved in 1 L dH_2O; kept at RT.

Table 2.6: List of buffers for chromatography

Description	Use	Content
Equilibration buffer	Glutathione Sepharose (GS) affinity chromatography	10 x PBS stock solution was diluted to 1 x PBS pH 7.4.
Wash buffer		
HRV-3C protease buffer		
Equilibration buffer	Ni-NTA affinity chromatography	20 mM Tris-HCl pH 8.0, 500 mM NaCl and 10 mM imidazole.
Wash buffer		20 mM Tris-HCl pH 8.0, 500 mM NaCl and 10 mM imidazole.
Elution buffer		20 mM Tris-HCl pH 8.0 with 500 mM NaCl and 200 mM imidazole.
Buffer	Size exclusion chromatography	1 x PBS pH 7.4.

Table 2.7: List of buffers and reagents for gel electrophoresis

Description	Content
Ammonium persulphate (APS)	10 % (w/v) APS in dH_2O; kept at 4 °C.
Tetramethylethylenediamine (TEMED)	100 % (w/v) TEMED
Resolving buffer	1.5 M Tris-HCl pH 8.8; kept at RT.
Stacking buffer	0.5 M Tris-HCl pH 6.8; kept at RT.
10 % (w/v) sodium dodecyl sulphate (SDS)	10 g of SDS dissolved in 100 mL dH_2O; kept at RT.
8 x SDS sample buffer	2.2 mL 0.5 M Tris-HCl pH 6.8, 4 mL 87 % (v/v) glycerol, 16 mL 10 % SDS, 200 µL β-mercaptoethanol, 0.8 % bromophenol blue; kept at 20 °C.
Coomassie staining solution	30 % (v/v) ethanol, 10 % (v/v) acetic acid, 0.25 % (w/v) Coomassie Blue R-250 in 50 % (w/v) dH_2O; kept at RT.
Destaining solution	Final concentrations: 40 % (v/v) of absolute ethanol, 10 % (v/v) of acetic acid glacial with 99.7 % purity and 50 % (v/V) dH_2O.
15 % SDS-PAGE Resolving gel	7.2 mL dH_2O, 7.5 mL 30 % (w/v) acrylamide, 5 mL 1.5 M Tris-HCl pH 8.8, 200 µL 10 % (w/v) SDS, 5 µL TEMED, 50 µL 20 % (w/v) APS.
5 % SDS-PAGE Stacking gel:	3.13 mL dH2O, 600 µL 30 % (w/v) acrylamide, 1.25 mL 0.5 M Tris-HCl pH 6.8, 75 µL TEMED, 12.5 µL of 10 % APS.

2.5 Bacterial vectors

Naturally occurring plasmids found in bacteria and other organisms are engineered to act as vectors. Plasmid vectors contain an origin of replication (ORI), drug-resistance gene, and a site for insertion of exogenous DNA fragments. Drug-resistance gene such as ampicillin-resistance gene (Amp^R) encodes β-lactamase, which inactivates the antibiotic ampicillin (Lodish et al., 2000). This allows bacterial cells that take up a plasmid to be selected for by growing them in the presence of an antibiotic such as ampicillin (Sambrook and Russell, 2001). pGEX-6P-1 and pET-21a are the two vectors used in this study. These vectors are represented in Figure 2.1 and summarized in Table2.8.

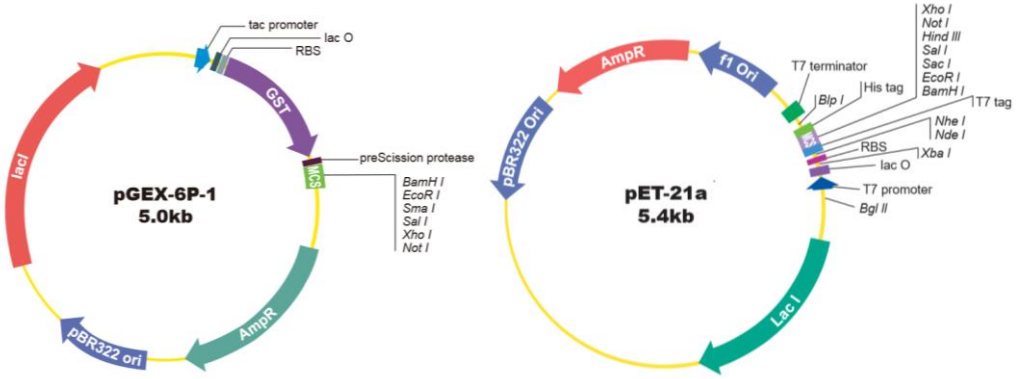

Figure 2.1: **Vector map of pGEX-6P-1 and pET-21a.**

The vector map of pGEX-6P-1 shows the important features of ampicillin resistance gene (Amp^R), tac promoter and glutathione S-transferase (GST) tag with multiple cloning site (MCS). The vector map of pET-21a shows the important features of ampicillin resistance gene (Amp^R), T7 promoter and C-terminal His_6 tag with multiple cloning site (MCS). Adapted from (Aatsinki and Rajaniemi, 2005)

Table 2.8: Summary of vectors used

Vector name	Plasmid type	Selectable marker	PreScission site	Protein purification tag	Size (kb)	Supplier
pGEX-6P-1	Bacterial expression	Ampillicin	HRV-3C cleavage sequence	GST-tag	4.9	GE Healthcare (Illinois, USA)
pET-21a	Bacterial expression	Ampillicin	None	His_6-tag	5.4	GE Healthcare (Illinois, USA)

2.6 Primer design

Primers with desired mutations needed to be incorporated in *Tuba SH3-6* gene were designed using QuikChange Primer Design guidelines. The guidelines included the following:

1. Both the reverse and forward primers needed to have the desired mutation.
2. Primers had to be between 25-45 bases long, with melting temperature (T_m) greater than or equal to 78 °C.
3. All desired mutations had to be approximately in the middle.
4. Primers had to be greater than or equal to 40 % of GC content and should end in one or more C or G bases.

In order to confirm that the primers fit the above guidelines, they were analysed by pasting into an online primer design program (https://depts.washington.edu/bakerpg/primertemp/). The outcomes from the program are shown in Table 2.9.

Table 2.9: List of primers for site-directed mutagenesis of Tuba SH3-6

Primer sequence and parameters (modified codons highlighted)	**Amino acid substitution**
Forward primer: 5'-GGCTACGTTCCCTCCAATGCGATCCGCAAAACCGAG-3' Reverse primer: 5'-CTCGGTTTTGCGGATCGCATTGGAGGGAACGTAGCC-3' Tm = 78.3 °C, Bases = 36, GC content = 58.3 %	Tyrosine 1570 to Alanine (Y1570A)
Forward primer: 5'-GTTACAGGAAATACAGAGGCGTGGTTAGCTGAGGTTAACGGG-3' Reverse primer: 5'-CCCGTTAACCTCAGCTAACCACGCCTCTGTATTTCCTGTAAC-3' Tm = 78.8 °C, Bases = 42, GC content = 50.0 %	Tryptophan 1554 to Alanine (W1554A)

Nucleotide bases highlighted yellow in Table 2.9 above are codons altered to incorporate mutations in *Tuba SH3-6* genes.

2.7 Making chemically competent *E. coli* cells

"Competent cells" allow incorporation of foreign DNA, by altering their cell membrane through a heat shock process. Chemically competent cells used in this study included *E. coli* DH5α and *E. coli* BL21, which were used for DNA propagation and protein production, respectively. Competent cells were made within three days using the $CaCl_2$ method.

Day 1: Frozen glycerol stocks from *E. coli* DH5α and BL21 cells were streaked out individually onto fresh agar plates without ampicillin. The plates were incubated at 37 °C overnight.

Day 2: A single colony of DH5α and BL21 cells was picked from the agar plates for inoculation into 25 mL of LB and grown overnight at 37 °C and 160 rpm in a shaking incubator (Multitron, Bottmingen, Switzerland). The following stock solutions were prepared: 100 mL of 500 mM $MgCl_2$, 100 mL of 500 mM $CaCl_2$, 50 mL of 100 % glycerol, 500 mL of 500 mM KCl, and 70 mL of 100 mM piperazine-N, N'-bis (pH 6.7). The stock solutions were used to make transformation buffer (TB) consisting of 22 mL of 55 mM $MgCl_2$, 6 mL of 15 mM $CaCl_2$, 100 mL of 250 mM KCl

and 20 mL of 70 mM piperazine-N, N'-bis (pH 6.7), and topped up to 200 mL with ddH_20. Both stock solutions and TB were kept overnight at 4 °C.

Day 3: The 25 mL pre-cultures were inoculated into separate flasks with 500 mL LB media and grown in a 37 °C shaking incubator at 190 rpm. Optical densities at 600 nm (OD_{600}) of growing cultures were determined (Cell Density Meter CO 8000, Cambridge, United Kingdom) at regular intervals until an early mid-log phase (OD_{600} = 0.4-0.7) was reached. Thereafter, cultures were transferred into clean autoclaved 1 L harvesting bottles. An F9-6 x 1000 LEX rotor was pre-cooled to 4 °C in a Sorvall Lynx 6000 centrifuge (Thermo Scientific, Massachusetts, USA). Each culture was centrifuged at 11 000 x *g* for 10 min at 4 °C. Cells were kept on ice and resuspended in 175 mL transforming buffer (i.e. at a ratio of 35 mL TB per 100 mL cell culture). The cells were placed on ice for 15 min. Thereafter, the cells were centrifuged at 11 000 x *g* for 10 min at 4 °C, resuspended in 10 mL of TB, centrifuged for 5 min at 4500 x *g* and resuspended in a buffer consisting of 8 mL 100 mM $CaCl_2$ and 2 mL 100 % glycerol. The resuspended cells were placed on ice and 50 µL aliquots transferred to sterile 1.5 mL tubes, cryocooled in liquid nitrogen and stored at -80 °C.

2.8 Transformation of competent cells

Transformation implicates a bacterium adopting genes from the external environment and acquiring new genetic makeup. Heat-shock and electroporation are methods used to transform chemical and electro-competent cells, respectively. In heat-shock, elevated temperature creates pores and permits genetic material to pass through bacterial membrane. Whereas, electroporation uses electrical pulses to allow genetic material entry (Green and Rogers, 2013, Dower *et al.*, 1988). Cells were induced to take up endonuclease-resistant plasmids (PCR products from site-directed mutagenesis) by heat-shock transformation. This was achieved by adding 5 µL of plasmid DNA to 50 µL of competent cells and placing the mixture on ice for 30 min. The cell/plasmid mix was transferred to a Thermomixer 5436 (Eppendorf, Hamburg, Germany) at 42 °C for 90 s, whereupon 800 µL pre-warmed LB was added and the tubes shaken on the Thermomixer 5436 (Eppendorf, Hamburg, Germany) at 37 °C for 1 h. Thereafter, 50 µL of the cells were transferred to a petri dish containing LB agar with 100 µg/mL ampicillin by

spreading using glass beads. The plates were incubated at 37 °C overnight. Colonies that grew on these plates were used in plasmid DNA isolation.

2.9 Plasmid DNA isolation

Resultant single colonies from transformation were picked and inoculated into 10 mL LB with 100 µg/mL ampicillin. The bacterial culture in a 50 mL tube was grown overnight at 37 °C in a shaking incubator at 190 rpm (Multitron, Bottmingen, Switzerland). Plasmid DNA was isolated from the overnight culture using the GeneJET plasmid mini-prep kit (Thermo Fisher Scientific, Massachusetts, USA), containing resuspension buffer, neutralisation buffer, spin columns, wash solution and elution buffer. Plasmid DNA was harvested through centrifugation. The cell pellets were resuspended in 250 µL resuspension buffer, before adding 350 µL neutralisation buffer. The solution was centrifuged at 10 000 x *g* for 5 min at 4 °C to remove chromosomal DNA and cell debris in the pellet from the supernatant. The latter was transferred to a GeneJET spin column and centrifuged at 10 000 x *g* for 1 min at 4 °C. The flow through was discarded. Wash solution of 500 µL was added to the column followed by centrifugation at 10 000 x *g* for 1 min at 4 °C. The flow through solution was decanted and this step was repeated. To get rid of ethanol in the wash solution, the column was further centrifuged at 10 000 x *g* for 2 min at 4 °C to cause ethanol evaporation before placing the column in an autoclaved 1.5 mL tube. To obtain the plasmid DNA, 50 µL of elution buffer was added to the column and centrifuged. The purified plasmid DNA concentration was measured using a Nanodrop ND-1000 spectrophotometer (Thermo Fisher Scientific, Massachusetts, USA) and stored at -20 °C for downstream experiments.

2.10 Site-directed mutagenesis of *Tuba SH3-6*

Site-directed mutagenesis (SDM) is a method used for introduction of specific mutation in a double-stranded DNA. Mutations are introduced by using primers with desired mutations in a PCR to amplify a plasmid template (Holland *et al.*, 2015). Parent plasmid DNA from bacteria having methylated DNA gets removed by DpnI (endonuclease). Whereas, the DNA amplified by PCR remains due to lack of methylated DNA (Lu *et al.*, 2002).

SDM was employed to help understand the relevance of specific residues of Tuba SH3-6 in relation to its physiological binding partner N-WASP and listerial InlC. Desired mutations were incorporated into *Tuba SH3-6* by using designed primers (Table 2.9) in a PCR. Reagents and PCR conditions are listed below in Table 2.10 and Table 2.11, respectively. To obtain a plasmid with the desired mutation, 45 µL of the PCR product was transferred into a 1.5 mL tube. The naturally methylated parental plasmid was digested with 10 U/µL DpnI enzyme for 1 h at 37 °C, whilst the non-methylated plasmid with the desired mutation remains.

Table 2.10: Reaction mixture for site-directed mutagenesis PCR

Reagent	**Volume**
5x Reaction buffer	10 µL
10 mM dNTPs	0.5 µL
10 µM forward primer	1 µL
10 µM reverse primer	1 µL
Template DNA (Tuba SH3-6)	0.5-1 µL
Phusion Hot Start II DNA polymerase (2 U/µL)	0.5 µL
MilliQ water	Top-up to 50 µL

Table 2.11: PCR conditions used in site-directed mutagenesis

Cycling step	**Temperature**	**Time**
Step 1: Initial Denaturation	98 °C	30 s
*Step 2: Denaturation	98 °C	10 s
*Step 3: Extension	72 °C	3 min
*Step 4: Final Extension	72 °C	10 min
Step 5: Hold	4 °C	∞

*Step 2 to 4 were repeated 32 times

2.11 Sanger sequencing

Sanger sequencing is an *in-vitro* method used to identify sequence and composition of DNA molecules. In this method, a double-stranded DNA is initially denatured to allow primer annealing. A mixture of deoxynucleotide triphosphates, comprising of arginine, guanine, tyrosine, and cytosine serve as building blocks for primer elongation to create a new double-strand DNA. Whereas, attachment of dideoxynucleotide triphosphates (ddNTPs) with fluorescent markers enable termination and visualization of sequence (Dean and Farmer, 2017). In order to verify if the correct mutations were incorporated, isolated recombinant DNA plasmids were sequenced by Sanger sequencing and analysed at an in-house sequencing facility. The gene section that needed to be sequenced was amplified through sequencing PCR using pGEX universal primers (Table 2.12) and reagents listed in Table 2.13. The "Big Dye" consist of dNTPs, *Taq* DNA polymerase and ddNTPs needed for amplification and termination processes in Sanger sequencing.

Table 2.12: Primers for Sanger sequencing experiments

Primer name	**Sequence**
pGEX (forward primer)	5' GGGCTGGCAAGCCACGTTTGGTG 3'
pGEX (Reverse primer)	5' CCGGGAGCTGCATGTGTCAGAGG 3'

Table 2.13: Sanger sequencing PCR reaction mixture

Reagent	**Concentration**	**Volume (µL)**
Plasmid DNA	60-100 ng	1 µL
Big Dye	-	1 µL
Primer	3.2 pmol	1 µL
Sequencing buffer (5X)	0.5 X	2 µL
MilliQ water	-	Top-up to 10 µL

PCR product from sequencing PCR was “cleaned up” through ethanol precipitation to remove NTPs, *Taq* DNA polymerase, primers and primer dimers, which may interfere with sequence result. This was achieved by adding reagents (Table 2.14) and centrifuging (Eppendorf microcentrifuge 5417 refrigerated, Hamburg, Germany) the sequencing PCR product for 30 min at 15000 x *g*. The supernatant was discarded gently, and precipitated DNA was washed twice with 70 % ethanol. To allow excess ethanol to evaporate, the samples were dried in the laminar flow cabinet for 30 min. Thereafter, the samples were ready to be analysed at an in-house sequencing facility.

Table 2.14: Reagent for PCR product precipitation

Reagent	Concentration	Volume
Sodium acetate (NaOAc)- pH 4.6	5 M	3 µL
99.9 % Ethanol	-	62.5 µL
MilliQ water	-	14.5 µL

2.12 Production of Tuba SH3-6 and InlC

After mutations had been confirmed by Sanger sequencing, *E. coli* BL21 cells were induced to take up recombinant plasmids encoding for wild-type and variants of Tuba SH3-6, and wild-type InlC by heat-shock transformation. Transformed cells were spread onto agar/ampicillin plates and incubated overnight at 37 °C. Single colonies from each plate were picked and inoculated into 25 mL LB with ampicillin. The cultures were grown at 37 °C overnight in a shaking incubator. Overnight starter cultures were added to 1 L LB/ampicillin media and grown at 37 °C till an OD_{600} of 0.6 to 0.8 was reached. A sample of 20 µL of the culture was transferred into a 1.5 mL tube and kept for SDS-PAGE analysis. Protein production was induced with 0.1 mM IPTG and further grown at 25 °C overnight. A sample of 20 µL of the induced overnight culture was transferred into a 1.5 mL tube and kept for analysis by SDS-PAGE. The 1 L cell cultures were harvested by pouring into centrifugation bottles and centrifuged at 4 °C for

15 min at 5000 x *g* using a F9-6 x 1000 LEX rotor in a Thermo Scientific Sorvall Lynx 6000 Centrifuge. The supernatants were discarded as waste and the cell pellets with the target protein were re-suspended in 20 mL 1 x PBS pH 7.4 and transferred into a 50 mL tube. To release soluble proteins, the harvested cells were lysed by sonicating (QSonica, Connecticut, USA) for 5 cycles with 30 s pulses at 30 % amplitude interspersed with 30 s breaks. To separate the soluble protein containing fraction (supernatant) from the insoluble membranes (pellet), the cell lysate was centrifuged in a 20 mL tube at 37 000 x *g* for 1 h at 4 °C using a F21-8 x 50y in a Thermo Scientific Sorvall Lynx 6000 centrifuge. A 20 µL sample of the insoluble fraction and soluble fraction was transferred into two separate 1.5 mL tubes for analysis by SDS-PAGE.

2.13 Protein purification by chromatography

Chromatography allows target proteins to be separated from other substances based on their unique properties such as ligand recognition, metal ion binding, size or charge. Mostly, affinity chromatography is used as a first step in the purification process followed by other purification method such as size exclusion chromatography (size) and ion exchange chromatography (charge) if the need arises to remove other impurities.

2.13.1 Glutathione Sepharose (GS) affinity chromatography

Tuba SH3-6 variants were purified by two step purification procedure. The GST tagged proteins were first purified from other impurities by GS affinity chromatography. To achieve this, 4 mL of glutathione sepharose (GS beads) were added to a column to allow flow through of 20 % ethanol, used to store the GS beads. The beads were equilibrated with 20 mL of 1 x PBS pH 7.4. The soluble protein described above was mixed with the GS beads in a 50 mL tube. For effective coupling, the beads/protein mix in a 50 mL tube was placed on a roller mixer SRT6 (Stuart Scientific, Staffordshire, UK) for 5 h at 4 °C. The beads/protein mix were transferred into a 10 mL column to allow unbound cellular proteins flow through by gravity into a 50 mL tube. For SDS-PAGE analysis, a sample of 20 µL of the flow through was transferred into a 1.5 mL tube. Unbound proteins were further washed from the beads-GST/fusion protein by gravity flow with 500 mL 1 x PBS pH 7.4. For SDS-PAGE analysis, a sample of 20 µL of the washed fraction was transferred into a 1.5 mL tube. Following the wash step, the beads-GST/fusion protein was

mixed with 10 mL 1 x PBS pH 7.4 by inverting the column gently. To cleave the target protein from GST, 50 mL of 50 mg/mL HRV-3C protease was added and placed on a roller mixer SRT6 (Stuart Scientific, Staffordshire, UK) overnight at 4 °C. Samples of both before and after HRV-3C protease cleavage were transferred into a 1.5 mL tubes for SDS-PAGE analysis. To elute the target protein, the 10 mL overnight cleavage solution was poured into a 10 mL column and the flow through was collected into a 15 mL tube. This flow through represents elution 1. Another 10 mL PBS was added to the same column and the flow through was collected into a 15 mL tube. The flow through in this case represents elution 2. Similarly, final elution in a 15 mL tube was obtained. After the final elution, a 20 µL sample of the beads were transferred into a 1.5 mL tube for SDS-PAGE analysis. The three elution fractions were pooled together and concentrated using centrifugal filters of 5 kDa MWCO (Merck, Darmstadt, Germany).

2.13.2 Immobilized metal affinity chromatography (IMAC)

His_6-InlC fusion protein was purified by IMAC. To achieve this, 4 mL of chelating agarose beads charged with Ni^{2+} ions were added into a 10 mL column and equilibrated with 50 mL of wash buffer (20 mM Tris-HCl pH 8.0 with 500 mM NaCl and 10 mM imidazole). The soluble InlC extract described above was added to the beads in a 50 mL tube. For effective coupling, the beads/protein mix in a 50 mL tube was placed on a roller mixer SRT6 (Stuart Scientific, Staffordshire, UK) for 5 h at 4 °C. The beads/protein mix was transferred into a 10 mL column to allow unbound cellular proteins to flow through by gravity into a 50 mL tube. For SDS-PAGE analysis, a sample of 20 µL of the flow through was transferred into a 1.5 mL tube. The unbound proteins were further washed from the beads/protein mix was washed by gravity flow with 500 mL wash buffer. For SDS-PAGE analysis, a sample of 20 µL of the washed fraction was transferred into a 1.5 mL tube. Following the wash step, the target protein was eluted using 20 mM Tris-HCl pH 8.0 with 500 mM NaCl and 200 mM imidazole (elution buffer). Three elution fractions - containing 10 mL per fraction – were collected into 15 mL tubes. Due to SDS-PAGE analysis, 20 µL of each elution fraction was transferred into a 1.5 mL tube.

2.13.3 Size exclusion chromatography of Tuba and InlC

The elution fractions described above from GS affinity chromatography and IMAC were concentrated to around 30 mg/mL. To confirm HRV-3C protease cleavage, the concentrated protein sample was analysed by SDS-PAGE. The cleaved target protein (Tuba SH3-6) mostly co-eluted with GST and other contaminants. These impurities were further separated from target protein by size exclusion chromatography using ENrich SEC 70 10/300 column connected on an automated liquid chromatography system, ÄKTA 900 (GE Healthcare, USA). Buffer exchange of InlC using size exclusion chromatography was necessary to keep protein in similar buffer as Tuba SH3-6. To equilibrate the column, 1 x PBS pH 7.4 was used. The mobile phase consisted of 1 x PBS pH 7.4 with of 0.2 mL/min flow rate. Elution fraction size of 1 mL was collected with absorbance measured at 280 nm. To ascertain target protein purity, peak fractions from size exclusion chromatography corresponding to proteins were analysed by SDS-PAGE.

2.14 Protein analysis by SDS-PAGE

Samples from elution peaks and proteins among complex extracts were analysed by SDS-PAGE. SDS-PAGE system consists of a resolving and stacking gel. The resolving gel resolves proteins based on their molecular weights (MWs) whilst the stacking gel concentrates proteins before it reaches the resolving gel. Protein samples were mixed with 8 x SDS sample buffer in 1.5 mL tubes at a 6:1 ratio. The sample buffer contains a reducing agent, β-mercaptoethanol to cleave disulphide bonds and SDS, an ionic detergent, which denatures proteins and provides an overall negative charge to proteins in proportion to their mass. The proteins acquire consistent mass to charge ratio and are separated by size as they move through a polyacrylamide matrix (He, 2011). To further denature protein samples, the protein/sample buffer mix in 1.5 mL tubes was placed on a Thermomixer 5436 Eppendorf (Hamburg, Germany) at 95 °C for 5 min. Thereafter, the protein samples and molecular weight marker (Thermo Fisher Scientific) were loaded in wells of 15 % SDS-PAGE. To resolve protein samples, Mini-PROTEAN (Bio-Rad, California, USA) power supply was turned on at 40 mA for 30 min. The gel was removed from glass plates and stained in Coomassie Brilliant Blue R250 staining solution for 10 min. To remove excess stain, the stained gel was first rinsed with water and further soaked in destaining solution, permitting

visibility of protein bands. By using Molecular Imager GelDoc XR (Bio-Rad, California, USA), images of gels were taken.

2.15 Biomolecular interaction studies

Biomolecular interaction techniques including isothermal titration calorimetry (ITC), surface plasmon resonance (SPR), microscale thermophoresis (MST) and biolayer interferometry (BLI) are usually exploited to investigate the binding affinity, kinetics and thermodynamics of biomolecular interactions. These techniques simply indicate whether two proteins/molecules are binding and not necessarily where the binding occurs. Using one of these techniques makes it possible to identify ligands/proteins that form complexes for subsequent experiments like co-crystallization (Tounge and Parker, 2011). ITC is a quantitative tool used to investigate thermodynamic properties when ligands/proteins interact. It is considered a gold standard technique because parameters such as affinity constant, stoichiometry, and enthalpy and entropy can be quantified in a single experiment without labelling the binding partner. Ligand titration into a sample cell with biomolecule of interest causes heat to be absorbed or released in a binding event. The heat change detected during a binding event is measured by a microcalorimeter.

2.15.1 Isothermal Titration Calorimetry (ITC) experiment

The binding affinities of Tuba SH3-6 / InlC and Tuba SH3-6 / N-WASP were investigated by ITC experiments. ITC experiments were conducted using MicroCal ITC_{200} with Origin v7.0 software (GE Healthcare, Illinois, USA). To prevent contaminants from previous runs, both the sample cell and titrating syringe were thoroughly washed 4 x with ddH_2O and further washed 1 x with protein buffer.

Tuba SH3-6 / N-WASP

In Tuba SH3-6 / N-WASP ITC experiments, SH3-6 variant protein and N-WASP were the target sample and ligand, respectively. To avoid air bubbles, the target sample (Tuba SH3-6) was pipetted gently into the sample cell. The ligand (N-WASP) was aspirated into the syringe and followed by 2 x purge-refill cycle to remove bubbles. The MicroCal ITC_{200} (GE Healthcare, Illinois, USA) was set as follows: cell temperature: 25 °C, initial delay: 120 s, reference power: 6 µcal/s,

stirring speed: 300 rpm, duration: 0.8 s, spacing: 120 s, filter period: 5 s, first injection volume: 0.4 µL.

Tuba SH3-6 / InlC

Similarly, in Tuba SH3-6 / InlC ITC experiments, SH3-6 variant protein and InlC were the target sample and ligand, respectively. The MicroCal ITC_{200} was set as follows: cell temperature: 25 °C, initial delay: 120 s, reference power: 6 µcal/s, stirring speed: 300 rpm, duration: 0.8 s, spacing: 120 s, filter period: 5 s, first injection volume: 0.4 µL.

2.16 X-ray crystallography

Vapour diffusion is a widely used protein crystallization method compared to batch and dialysis (Chayen and Saridakis, 2008). For vapour-diffusion method (Figure 2.2), a drop consisting of protein and reservoir solution are mixed to have a lower concentration, relative to the reservoir solution alone. The mixture is placed near the reservoir solution containing non-volatile precipitant and high concentration of salts (Dessau and Modis, 2011). Due to osmotic pressure differences in the two solutions (drop and reservoir), water diffuses from the drop into the concentrated reservoir solution. This diffusion leads to slow decrease in volume and increased concentration of the drop, resulting in supersaturation for nucleation of protein crystals to form (Bolanos-Garcia and Chayen, 2009). Often, a 1:1 ratio of protein to reservoir solution is mixed. The drop mixture is placed on a cover slip or drop support near the vicinity of the reservoir solution, depending on whether it is a hanging-drop (Figure 2.2 A)) or sitting-drop (Figure 2.2 B)) experiment. Prior to the crystallization experiments, the best protein complex samples of 20 mg/mL were selected.

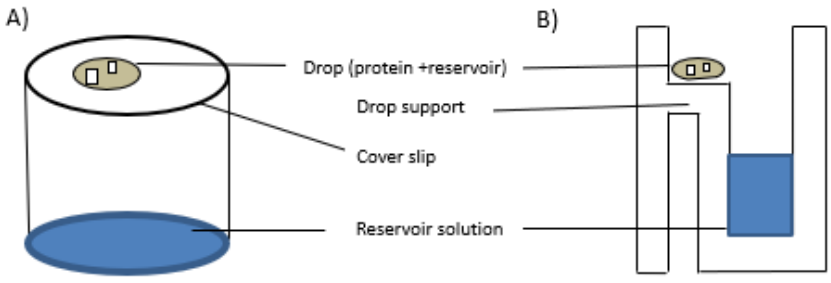

Figure 2.2: **Schematic diagram of protein crystallization methods**.
Crystallization using hanging-drop (A) or sitting-drop (B) vapour diffusion method. Adapted from (Dessau and Modis, 2011).

2.16.1 Crystallization of Tuba SH3-6 / N-WASP Complex

Variants of Tuba SH3-6 (Y1570A and W1554A) that had reduced affinity for InlC relative to N-WASP, were co-crystallized with N-WASP. The chemically synthesized N-WASP peptide was dissolved in ddH_20 and mixed in a 1.5 mL tube with variants of Tuba SH3-6 in 3:1 ratio for 1 hr incubation at 4 °C. To crystalize protein complexes, both hanging-drop and sitting-drop crystallization experiments were also set up. Previous conditions of 2 M NaCl, 0.1 M Bis-Tris pH5.5 (Polle *et al.*, 2014), that successfully produced Tuba SH3-6 / N-WASP crystals were used in the hanging-drop experiment. The experimental set up was in a 24-well hanging drop vapour diffusion plate consisting of 2 µL reservoir and 2 µL complex protein (20 mg/ mL). Commercial Hampton Index TM HR2-144 screens were used in 96-well sitting drop vapour diffusion plates using 2 µL reservoir and 2 µL protein (20 mg/ mL).

2.16.2 Crystallization of Tuba SH3-6 / InlC complex

Variants of Tuba SH3-6 (N1535A and E1575A) with weakened affinity for N-WASP relative to InlC, were co-crystallized with InlC. Tuba SH3-6 and InlC were mixed in a 1.5 mL tube in 1:1.5 ratio for 1 h incubation at 4 °C. To crystalize protein complexes, both hanging-drop and sitting-drop crystallization experiments were set up. Previous conditions of 1.6 M $NaKHPO_4$, 0.1 M HEPES pH 7.5 (Polle *et al.*, 2014) that successfully produced Tuba SH3-6 / InlC crystals were used in the hanging-drop experiment. The experimental set up was in a 24-well hanging drop vapour diffusion plate consisting of 2 µL reservoir and 2 µL complex protein (20 mg/mL). Commercial Hampton Index TM HR2 144 screens were used in 96-well sitting drop vapour diffusion plates using 2 µL reservoir and 2 µL protein (20 mg/ mL).

2.16.3 Data collection and structure determination

To prevent crystalline ice, the crystals obtained were cryocooled through 'fishing' and transferring them into a solution consisting of reservoir solution and 25 % glycerol before sending them to Diamond, UK for X-ray diffraction and data collection. The crystals were remotely analysed and data sets were collected on beamline IO3 (Diamond, UK). The diffraction data was processed on autoPROC, solved through molecular replacement (PHENIX) by using Tuba SH3-6 / InlC complex (PDB code: 4CC4), a structure solved by Polle *et al.*, 2014 as a search model with 98 % sequence identity. Using PHENIX autobuild and refinement routines, a model

was built from electron-density maps generated from the diffraction patterns. For improved refinement, the model was manually rebuilt using WinCoot and PHENIX refine routines. Finally, the structure was analysed using PyMol (DeLano, 2002).

3 Results

3.1 Tuba SH3-6 variants constructed by mutagenesis

To abrogate the interaction of the Tuba SH3-6 domain with either InlC or N-WASP, variants of Tuba SH3-6 were constructed by introducing a single point mutation into the Tuba SH3-6 encoding gene. Targeted residues included asparagine 1535, glutamate 1575, tyrosine 1570 and tryptophan 1554. All were replaced with alanine, yielding Tuba SH3-6 variants N1535A, E1575A, Y1570A and W1554A, respectively as shown in Figure 3.1 A) to D).

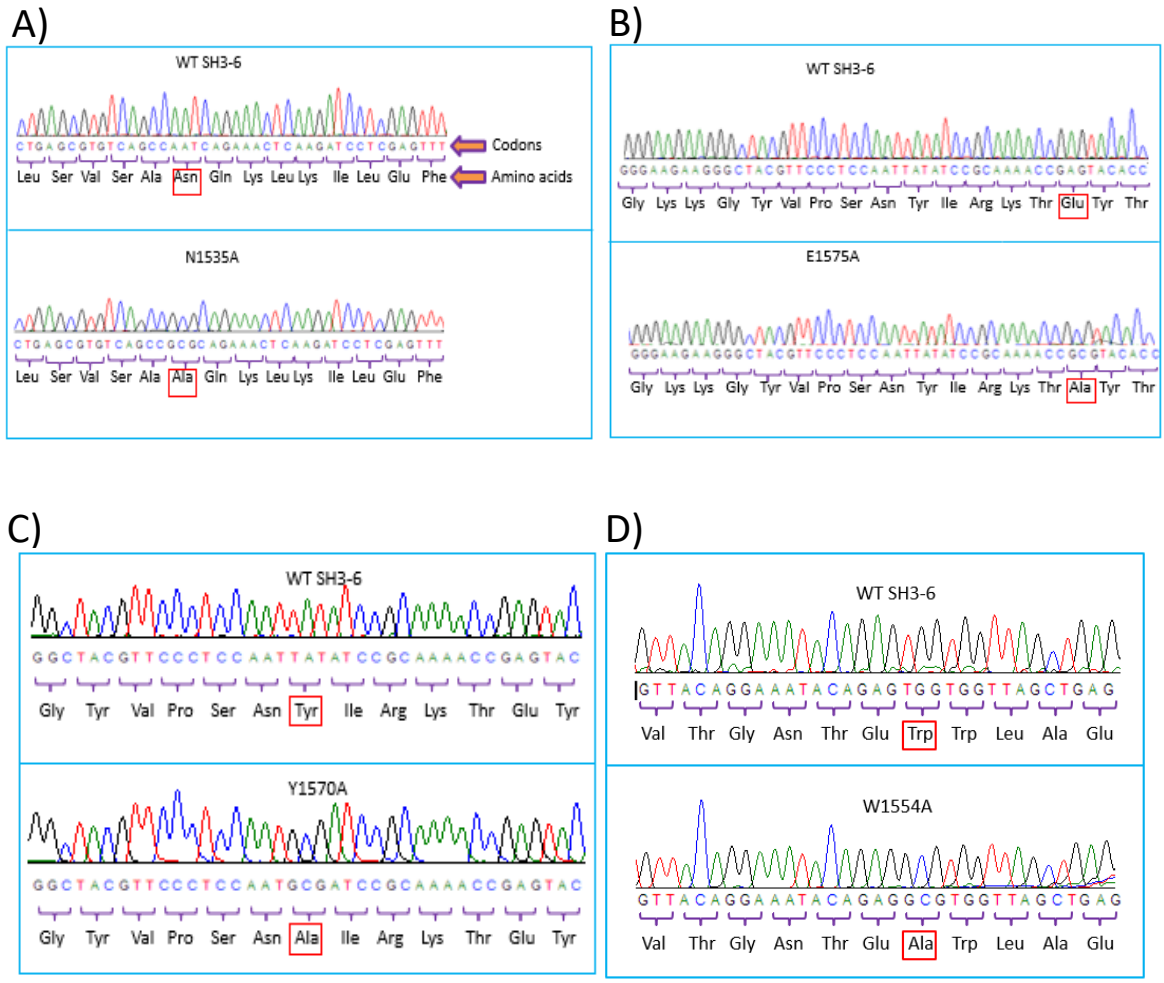

Figure 3.1: **Variants compared to wild-type *Tuba SH3-6* sequences**.
Variants of *Tuba SH3-6* were generated by site-directed mutagenesis. Sanger sequencing was used to confirm the mutations. In Figure 3.1 A) to D), the top and bottom sequences represent wild-type and variants of Tuba SH3-6, respectively. Codons corresponding to individual amino acids are shown in Figure 3.1 with specific codons altered to incorporate mutations. Amino acids replaced with alanine are highlighted by small red rectangular boxes.

3.2 Tuba protein production and GS-affinity chromatography

E. coli BL21 cells transformed using corresponding plasmids, were used to produce wild-type and variants of Tuba SH3-6. Cultures were grown in LB medium at 25 °C for 18 h after IPTG induction. GST-fusion proteins were purified using GS-affinity chromatography. SDS-PAGE analysis (Figure 3.2) below shows a typical wild-type or variant of Tuba SH3-6 production and GS-affinity purification.

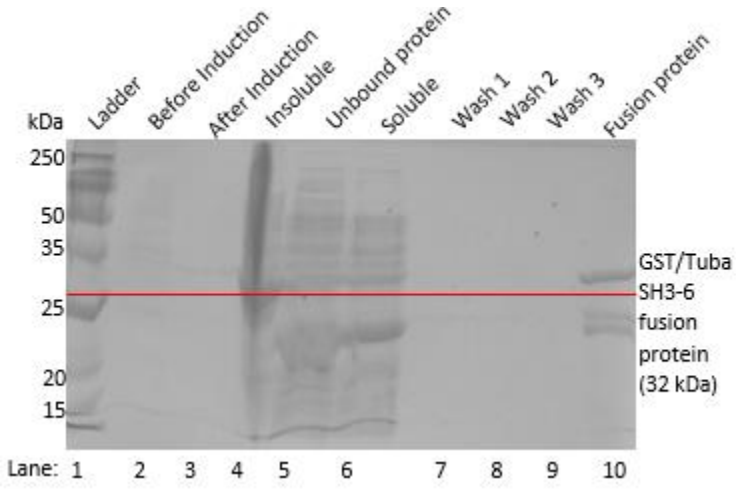

Figure 3.2: **SDS-PAGE of Tuba SH3-6 production and purification**.
Tuba SH3-6 was produced and first purified by GS affinity chromatography. The gel has a ladder/protein molecular weight marker at the far-left lane. Lanes 2 to 10 represent samples taken from before IPTG induction, after induction, insoluble, unbound protein, soluble, wash 1 to 3 and fusion protein fraction, respectively.

Lane 1 reveals the ladder/protein molecular weight marker, a combination of proteins of known molecular mass (kDa). The lowest and highest bands in this lane are 15 and 250 kDa, respectively. It indicates the relative molecular sizes of proteins analysed by SDS-PAGE. Lane 2 represents samples taken before IPTG induction, revealing no recognisable bands corresponding to the expected fusion protein. This is an indication that the system is efficiently controlled by IPTG induction to produce Tuba SH3-6. Lanes 3 to 6 reveal samples taken from after induction, insoluble, unbound protein and soluble fraction. These lanes reveal bands at around 32 kDa underlined in red. Bands at around 32 kDa correspond to GST-fusion protein of wild-type or variant Tuba SH3-6. It is an indication that after IPTG induction the target protein was successfully produced. Lanes 7 to 9 reveals samples taken from wash fractions. No recognisable bands are seen in these lanes. Thus, no unbound *E. coli* proteins were noticed in the wash fraction. Lane 10 reveals sample from coupling of the target protein to GS beads. The highest band in this lane is around 32 kDa underlined in red. The GS-affinity chromatography mostly yielded ~4 mg of GST-fusion proteins of wild-type or variant Tuba SH3-6 from 1 L of cell culture.

3.3 Size exclusion chromatography of Tuba SH3-6

Addition of 50 mg/mL HRV-3C protease to the beads-GST/fusion protein resulted in cleaved target protein (Tuba SH3-6) that co-eluted with GST. To separate Tuba SH3-6 from GST, elution fractions of Tuba SH3-6 were pooled (Figure 3.3 B, lane 2) and further purified by size exclusion chromatography (Figure 3.3 A). Figure 3.3 A) below is a chromatogram from size exclusion chromatography of Tuba SH3-6, which was analysed by SDS-PAGE as shown in Figure 3.3 B).

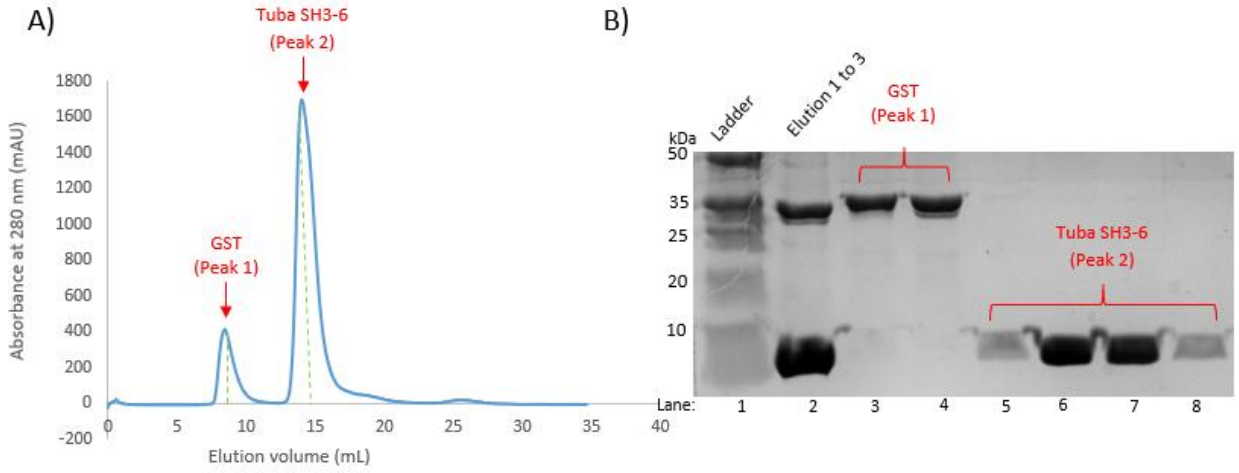

Figure 3.3: **Size exclusion chromatogram and SDS-PAGE analysis of Tuba SH3-6 after HRV-3C protease**.
A) Size exclusion chromatogram of Tuba SH3-6. Two prominent proteins were separated. B) SDS-PAGE analysis to confirm samples purity. Lane 1 reveals the ladder/protein molecular weight marker. In Lane 2 is the concentrated elution fractions of Tuba SH3-6 after GS affinity chromatography. Lanes 3 and 4 represent peak 1 from size exclusion chromatography, whilst lane 4 to 8 represent peak 2 from size exclusion chromatography.

The chromatogram of Tuba SH3-6 purification by size exclusion chromatography reveals two distinct peaks (Figure 3.3 A). The first peak is shorter with an elution volume of around 9 mL. A second longer peak with an elution volume of around 15 mL is also observed in the chromatogram. Both peaks suggest that two proteins were separated before one total column volume (24 mL) of buffer had passed through the column. In Figure 3.3 B), size exclusion chromatography fractions corresponding to the two different peaks were analysed by SDS-PAGE. The lane on the far-left reveals protein ladder. Lane 2 represents the concentrated elution fractions of Tuba SH3-6 before further purification by size exclusion chromatography. This lane contains two pronounced protein bands. The upper band between 25 and 35 kDa presumably corresponds to GST with molecular mass of around 26 kDa. We interpret the lower band below 10 kDa to be the target protein as its molecular mass is 7.5 kDa. Lanes 3 and 4 represent peak 1 from the size exclusion chromatogram. The bands correspond in size to GST (26 kDa). Lanes 5 to 8 represent peak 2 from size exclusion chromatogram. They correspond in size to the target protein Tuba SH3-6, which implies that it was successfully purified.

3.4 InlC production and purification

L. monocytogenes secretes InlC, which interacts with human Tuba SH3-6. InlC was produced by transforming *E. coli* BL21 strain with pET21a *inlC* plasmid and growing the resulting culture at 25 °C for 18 h after IPTG induction. The resulting InlC had a His_6-tag allowing it to be purified by IMAC. Samples saved during InlC production and purification were analysed by SDS-PAGE as shown below in Figure 3.4.

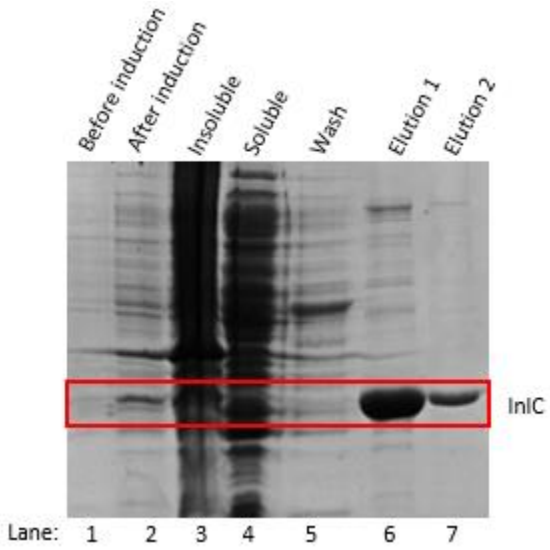

Figure 3.4: **SDS-PAGE analysis of InlC production and purification.**
The gel reveals sample taken from before IPTG induction, after induction, insoluble, soluble, wash, elution 1 and 2, respectively.

The lane on the far left represents a sample taken before IPTG induction. This lane reveals no recognisable bands corresponding to the expected protein. This is an indication that the system is efficiently controlled by IPTG induction to produce InlC. Lane 2 corresponds to a sample taken after induction. The bands are more prominent relative to lane 1 and a pronounced band was visible at around 29 kDa (red box), implying that InlC production was successfully induced at 25 °C. Lanes 3 and 4 represent samples from insoluble and soluble fractions. Continuous dark smears are observed in these lanes. This is due to very high-level protein expression in the inclusion bodies. The soluble fraction coupled to beads was washed to get rid of unbound proteins. Lane 5 reveals sample from wash fraction with recognisable bands. These bands correspond to unbound proteins after coupling soluble fraction to beads. Lanes 6 and 7 represent samples from elution fractions. Samples in these lanes had pronounced protein bands at the expected size of InlC as highlighted in the red rectangle. The impurities in lane 6 are consistent with those seen in lane 5. This indicates that a prolonged wash is needed before InlC is eluted from the column. The eluted fractions were pooled together and concentrated to approximately 20 mg/mL.

3.5 Size exclusion chromatography of InlC

Buffer exchange of InlC using size exclusion chromatography was exploited to keep InlC in similar buffer as Tuba SH3-6. The column was equilibrated with 1 x PBS pH 7.4.

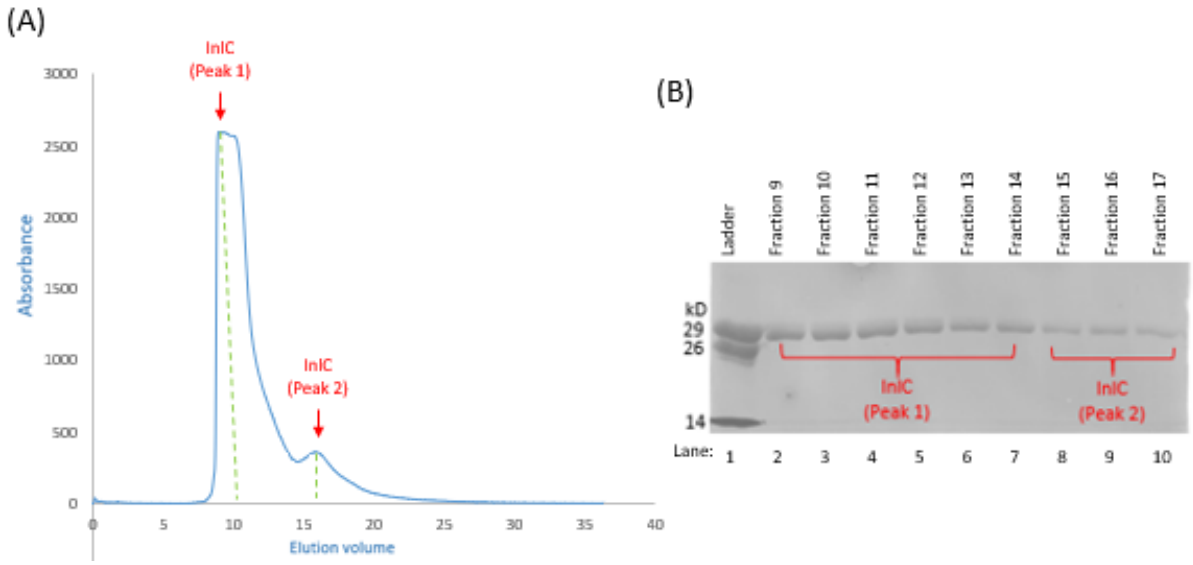

Figure 3.5: **Size exclusion chromatogram and SDS-PAGE analysis of InlC.**
A) Buffer exchange of InlC using size exclusion chromatography. Two peaks were observed. B) SDS-PAGE analysis to confirm InlC samples. Lane 1 contains mixture of GST (26 kDa), InlC (29 kDa) and lysozyme (14 kDa) used as a marker. Lanes 2 to 10 are fractions samples 9 to 17 from size exclusion chromatography.

The chromatogram (Figure 3.5 A) from size exclusion chromatography reveals two incompletely separated peaks at elution volumes of around 10 and 15 mL, respectively. This suggest that two proteins were separated before one total column volume (24 mL) of buffer had passed through the column. Fractions from the size exclusion chromatography were analysed by SDS-PAGE (Figure 3.5 B). The left-hand lane reveals a ladder consisting of previously purified GST (26 kDa), InlC (29 kDa) and lysozyme (14 kDa). Lanes 2 to 7 represent fraction samples 9 to 14 corresponding to peak 1. The pronounced protein bands observed in these lanes had a mass of around 29 kDa, corresponding to that of InlC. Lanes 8 to 10 display fraction samples 15 to 17 from peak 2. Also, these bands had a mass of around 29 kDa. A possible interpretation is that InlC forms both dimers and monomers.

3.6 ITC Analysis

The binding affinities between Tuba SH3-6 and its binding partners (InlC or N-WASP) were quantified by ITC experiments. During the ITC experiments, a ligand (either InlC or N-WASP) was titrated into a sample cell containing the target sample (Tuba SH3-6). The binding of the ligand to the target sample, resulted in heat release. In all the experiments, the binding reaction released heat indicating an exothermic reaction.

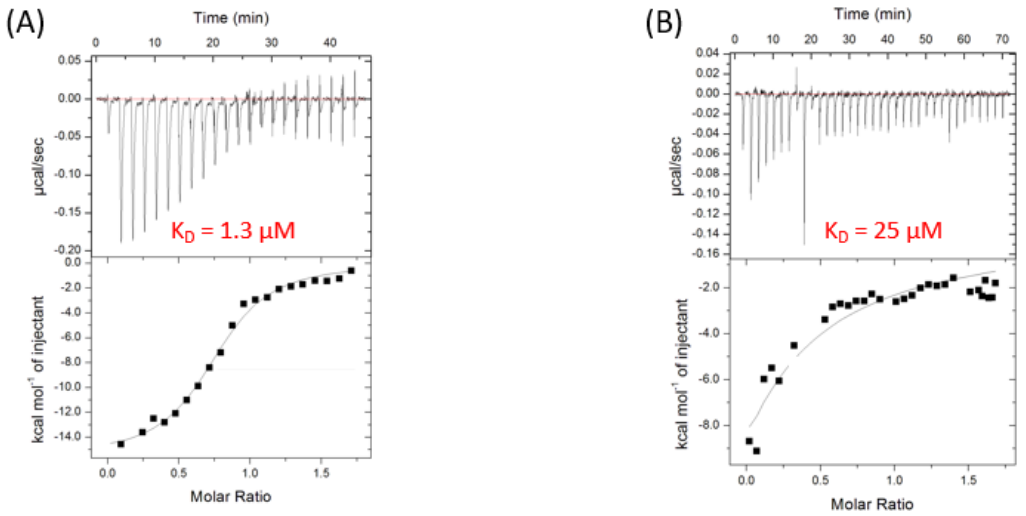

Figure 3.6: **ITC experiment for wild-type Tuba SH3-6 with InlC (A) and N-WASP (B)**.
The isotherms indicating interaction between proteins were in the upper panels. The lower panels display a plot of heat signal generated by the Origin v7 software.

The upper panels of Figure 3.6 display peaks corresponding to heat released during binding events. Negative peaks denote exothermic reactions. The lower panels display the integrated area of each peak associated with the titration process versus molar ratio of target protein to ligand. In Figure 3.6 (A), InlC with a concentration of 400 µM was titrated as 19 injections of 2 µL each into a sample cell containing 40 µM of Tuba SH3-6 wild-type. As more InlC is injected into the sample cell, temperature changes progressively decrease. The Tuba SH3-6 reaction reaches saturation within 19 injections. This matches the progressively shorter peaks in the upper panel. The lower panel has a sigmoidal curve, which indicates interaction between the two proteins with the correct concentration (i.e. 10 K_D > concentration in reaction vessel > 0.1 K_D). The curve was evaluated to yield a dissociation constant K_D = 1.3 µM.

In Figure 3.6 (B), 35 µL of 800 µM N-WASP were injected as 1 µL volumes into the sample cell containing 80 µM of wild-type Tuba SH3-6. As more N-WASP is injected into the sample cell, the amount of heat released decreases indicating the reaction to have been saturated. Plotting the integrated changes in heat against the stoichiometric ratio revealed an exponential curve rather than the expected sigmoidal, implying that the observed reaction is not the expected Tuba SH3-6 / N-WASP interaction. The most probable explanation is that the observed reaction is due

to the dissolution of N-WASP peptide dimers or higher oligomers that resulted from the very high concentration of peptide required to measure the low binding affinity of the complex. The apparent dissociation constant for this reaction was quantified as $K_D = 25$ µM. As the SH3-6 / N-WASP reaction is masked by the N-WASP oligomerisation, we conclude that the associated dissociation constant must be even higher than 25 µM.

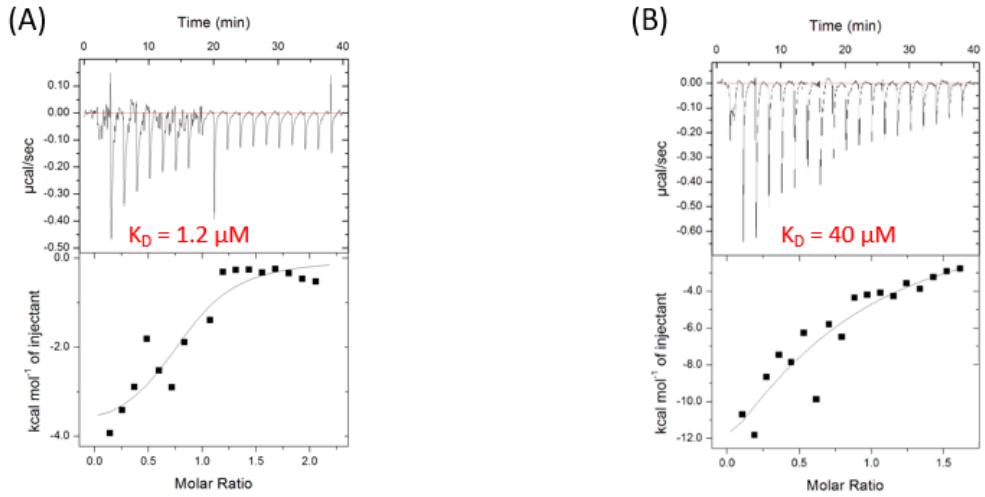

Figure 3.7: **ITC experiment for N1535A with InlC (A) and N-WASP (B)**.
Profiles similar to that observed in Figure 3.6 were obtained, but with more variation in the lower molar ratios.

Figure 3.7 reveals negative peaks denoting exothermic reactions. In Figure 3.7 (A), InlC with a concentration of 400 µM was titrated as 19 injections of 2 µL each into a sample cell containing 40 µM of Tuba SH3-6 variant N1535A. As more InlC is injected into the sample cell, temperature changes progressively decrease. The reaction reaches saturation within 19 injections. This matches the progressively shorter peaks in the upper panel. In this panel, some outliers complicate the interaction without invalidating the run. The curve is mostly sigmodal, similar to that observed for InlC binding wt Tuba in Figure 3.6 (A). The observed deviation of the inflection point from the known molecular ratio or 1:1 reflects minor pipetting errors that are not critical to the interpretation of the results. The curve in the lower panel was evaluated to yield a dissociation constant $K_D = 1.2$ µM.
In Figure 3.7 (B), 40 µL of 500 µM N-WASP were injected as 2 µL volumes into the sample cell containing 50 µM of Tuba SH3-6 variant N1535A. Similar to Figure 3.6 (B) with an exponential curve, the reaction here is also formation of N-WASP dimers or higher oligomers due to the high concentration of N-WASP. The apparent dissociation constant for this molecular interaction was quantified as $K_D = 40$ µM.

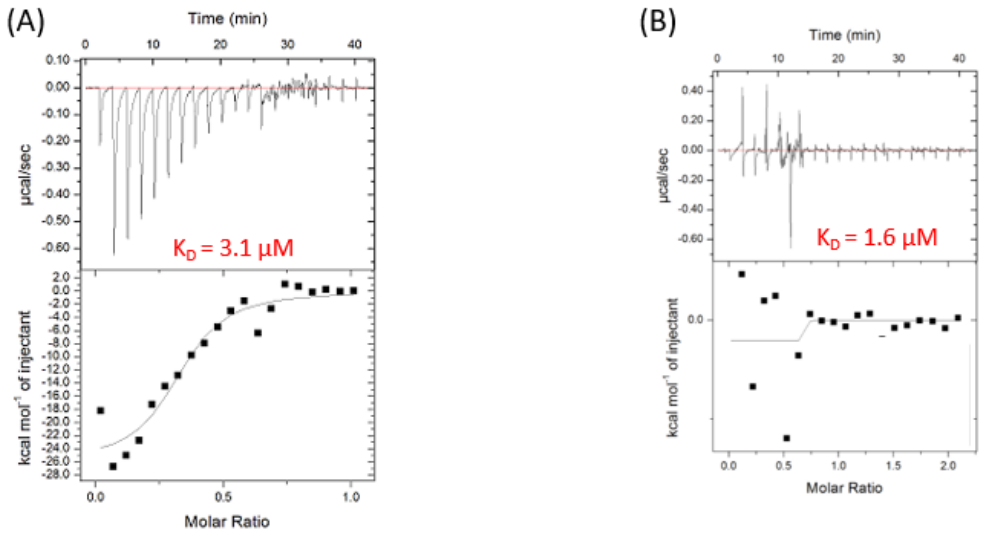

Figure 3.8: **ITC experiment for E1575A with InlC (A) and N-WASP (B)**.
Downward peaks and short even peaks are observed in experiment for E1575A / InlC (A) and E1575A / N-WASP (B), respectively.

In Figure 3.8 (A), titration of InlC into Tuba SH3-6 variant E1575A at similar concentrations as previous experiments caused saturation to be reached within 19 injections. In the upper panel are negative peaks denoting exothermic reaction. The lower panel has a curve mostly sigmoidal, which indicates interaction between the two proteins. The curve in the lower panel was evaluated to yield a dissociation constant K_D = 3.1 µM. In Figure 3.8 (B), 40 µL of 500 µM N-WASP were injected as 2 µL volumes into the sample cell containing 50 µM of Tuba SH3-6 variant E1575A. A step curve is witnessed in the lower panel for N-WASP into Tuba SH3-6 variant E1575A reaction. The step curve indicates interaction between the two proteins with high concentrations. The apparent dissociation constant for this molecular interaction was quantified as K_D = 1.6 µM.

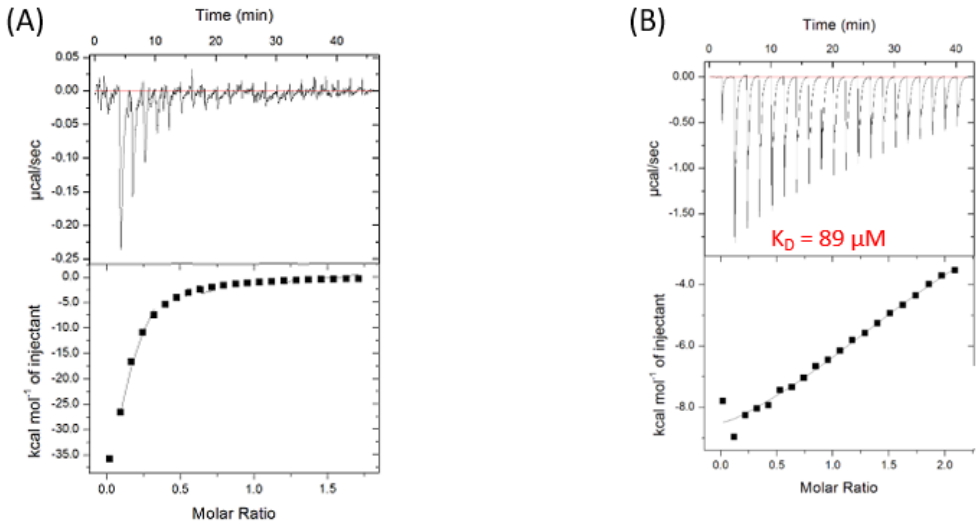

Figure 3.9: **ITC experiment for Y1570A with InlC (A) and N-WASP (B).**
In the experiment for Y1570A with InlC the peaks observed are not well defined. Exothermic reactions with downward peaks are observed in experiment for Y1570A with N-WASP.

In Figure 3.9 (A), InlC with a concentration of 400 µM was titrated as 19 injections of 2 µL each into a sample cell containing 40 µM of Tuba SH3-6 variant Y1570A. An exponential curve is observed in the lower panel. As explained for figure 3.6 (B), an exponential curve is most easily explained as resulting from the dissociation of the titrant – in this case InlC. InlC is known to dimerise (Polle *et al.*, 2014) and dimers are induced in this case by the high protein concentration and length of time that the InlC solution is incubated at this concentration.
In Figure 3.9 (B), 40 µL of 500 µM N-WASP were injected as 2 µL volumes into the sample cell containing 50 µM of Tuba SH3-6 variant Y1570A. The reaction here is also formation of N-WASP dimers or higher oligomers due to the high concentration. The apparent dissociation constant for this molecular interaction was quantified as K_D = 89 µM.

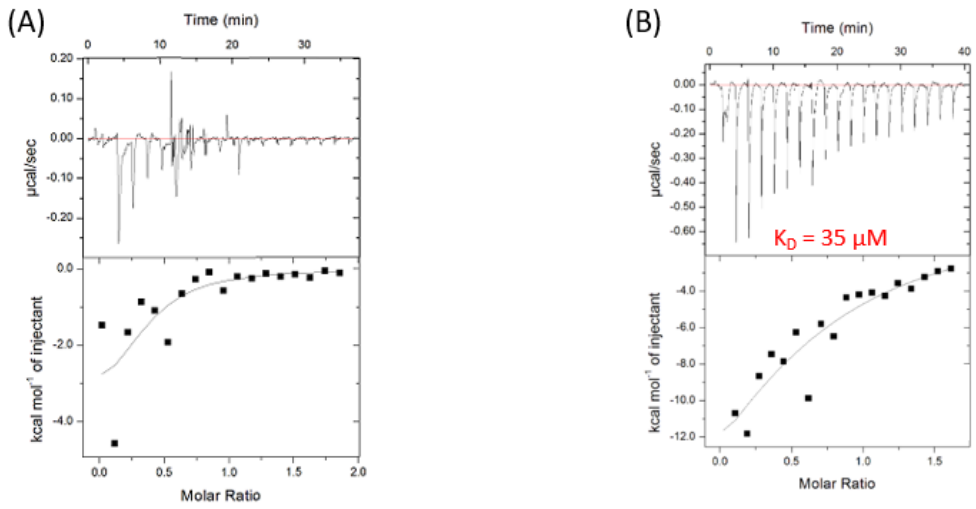

Figure 3.10: **ITC experiment for W1554A with InlC (A) and N-WASP (B).**
Poor peaks indicating no significant interaction are observed in experiment for W1554A with InlC. Exothermic reactions with downward peaks are observed in experiment for W1554A with N-WASP.

In Figure 3.10 (A), InlC with a concentration of 400 µM was titrated as 19 injections of 2 µL each into a sample cell containing 40 µM of Tuba SH3-6 variant W1554A. The lower panel shows a non-sigmoidal curve, similar to Figure 3.9 (A), the reaction occurring is simply separation of InlC dimers into monomers without any binding event since InlC tends to dimerize as known by (Polle *et al.*, 2014) and in Figure 3.5.
In Figure 3.10 (B), N-WASP with a concentration of 500 µM was titrated as 19 injections of 2 µL each into a sample cell containing 50 µM of Tuba SH3-6 variant W1554A. Similar to Figure 3.9 (B), the reaction here is also formation of N-WASP dimers or higher oligomers due to the high concentration. The apparent dissociation constant for this molecular interaction was quantified as K_D = 35 µM.

3.7 Co-crystallization of Tuba SH3-6 variant with either InlC or N-WASP

Tuba SH3-6 and its binding partner (InlC or N-WASP) were co-crystallized using either hanging-drop or sitting-drop method. However, InlC-only crystals appeared in the co-crystallization experiments. These crystals grew after three weeks at 4 °C. A sitting-drop reservoir solution consisting of 3M NaCl and 1M Bis-Tris pH 6.5 yielded the oval-shaped crystals (Figure 3.10) with maximum dimension of 755 µm. Crystals with different space groups ranging from $P2_12_12$, $P2_122$, $P222$, and $P1$ were obtained. However, the crystal that diffracted had a space group of $P2_12_12$ with a unit cell parameter of a = 58.8 Å, b = 178.8 Å, c = 42.7 Å. As indicated in Table 3.1, the total number of reflections and unique reflections were 78768 (7720) and 39384 (3860), respectively. Multiplicity was 2.0 with 100 % completeness. The Mean I/sigma(I), Wilson B-factor and R-merge were 8.27 (1.19), 15.52 and 3.79 (73.16), respectively.

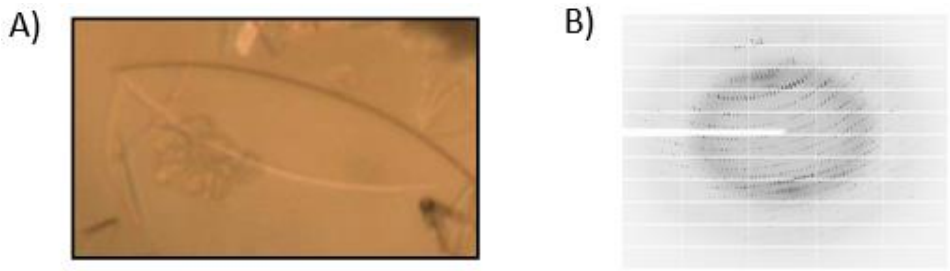

Figure 3.10: **Images of InlC crystal and diffraction pattern.**
A) An oval-shaped crystal resulting from reservoir solution of 3M NaCl and 1M Bis-Tris pH 6.5 in a sitting-drop experiment. B) X-ray diffraction of the crystal resulted in InlC diffraction pattern.

The table below (Table 3.1) provides a summary of data collected from the InlC crystal.

Table 3.1: Summarized data of InlC crystal

Data collection statistics	
Space group	$P2_12_12$
Unit cell (a,b,c,α,β,γ)	58.8 Å, 178.8 Å, 42.7 Å, 90°, 90°, 90°
Total reflections*	78768 (7720)
Unique reflections*	39384 (3860)
Multiplicity*	2.0 (2.0)
Completeness (%)*	99.94 (100.00)
Mean I/sigma(I)*	8.27 (1.19)
Wilson B-factor	15.52
R-merge* (%)	3.79 (73.16)

***Brackets indicate values for shell of highest resolution.**

3.7.1 Crystal structure of InlC

Molecular replacement was used to determine InlC crystal structure. This technique is ideal when crystal structures of homologs are available. In this case, a crystal structure at slightly lower resolution (PDB code: 1XEU) with 98 % sequence identity was used as the search model. Molecular replacement was achieved using Phaser (McCoy *et al.*, 2007). The resulting electron density maps were inspected using Coot (Emsley and Cowtan, 2004) and the model was improved manually. The improved model was refined, and the resulting statistics are listed in Table 3.2.

Table 3.2: Summarized refinement statistics of InlC crystal

Refinement statistics	
Resolution range*	42.7 - 1.85 (1.92 - 1.85)
Reflections used*	39381 (3860)
Reflections for R-free*	1970 (174)
R-work / R-free (%)*	22.9 (33.2) / 25.9 (34.4)
CC(work) / CC(free)*	0.91 (0.17) / 0.90 (0.12)
InlC atoms / residues	2080 / 263
Solvent molecules	314
RMS bonds (Å)	0.008
RMS angles (°)	1.26
Ramachandran: favoured, allowed, outliers (%)	94, 5, 1

***Brackets indicate values for shell of highest resolution**.

As expected, the solved crystal structure of InlC (Figure 3.11) in this study is closely related to that reported by Ooi *et al.*, 2006. It consists of 263 residues within three different domains: The N-terminal or cap domain (blue) encompasses residues 35 to 76 and consists of three α-helices and two short β-strands. The central LRR domain (green) encompasses residue 77 to 213. It takes the form of a right-handed superhelix comprising six repeats of 22 residues. Repeat three is an exception with only 21 residues. The C-terminal immunoglobulin (Ig)-like domain (orange) encompasses residues 207 to 297.

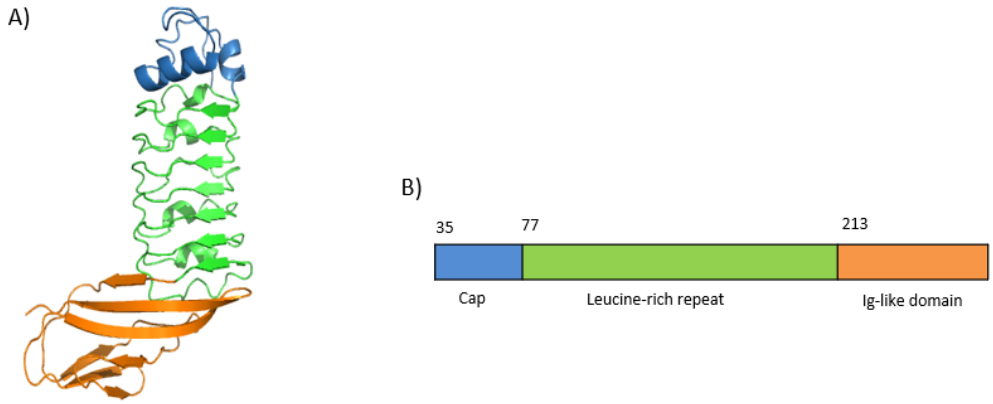

Figure 3.11: **Structure of InlC.**
A) A ribbon diagram of solved InlC structure, produced using PyMol (DeLano, 2002). B) Schematic diagram showing the different domains. The N-terminal cap domain (blue), the central LRR domain (green), and the C-terminal immunoglobulin (Ig)-like domain (orange).

4 Discussion

Invasion by microorganisms is normally prevented by barriers such as intestinal, fetoplacental and blood-brain barriers found in humans. However, pathogenic microorganisms have evolved mechanisms and specialized virulence factors that interact with host biomolecules to cross these barriers and spread in host cells (Doran *et al.*, 2013). Usually, virulence factors strongly bind to host biomolecules to disrupt native physiological interactions. For better insight on molecular basis of pathogenesis, it is critical to understand the nature and strength of molecular interactions (Alberts *et al.*, 2002). This study focused on the human protein Tuba and its physiological and pathological interaction partner human N-WASP and listerial InlC, respectively. It remains unclear whether other listerial factors also promote protrusion formation and cell-to-cell spread. Hence, this study aims to further understand how these processes work by developing variants of Tuba SH3-6 retaining affinity for either InlC or N-WASP but not the other for downstream analysis of cell-to-cell spread.

4.1 Site-directed mutagenesis of Tuba SH3-6

Site-directed mutagenesis (SDM) is a very useful technique in molecular biology and protein engineering, generating variant proteins suitable for biophysical and functional studies (Liu and Naismith, 2008). This technique was previously used by Polle *et al.* (2014) to generate variant proteins of Tuba SH3-6. In this study, variants of Tuba SH3-6 were achieved by SDM using PCR to amplify primers with the desired mutations. Prior to SDM, crystal structures of Tuba SH3-6 / InlC and Tuba SH3-6 / N-WASP complexes were visualized using three-dimensional graphics software, PyMol (DeLano, 2002). Here, the regions whereby Tuba SH3-6 exclusively binds to InlC or N-WASP were analysed to identify critical residues involved in the interactions. Critical residues of Tuba SH3-6 were identified and replaced with alanine to weaken the binding of one partner (either InlC or N-WASP) without affecting the other. Selectively weakening the interaction of Tuba SH3-6 with InlC allows Tuba to function independently of InlC, identifying potential alternative roles for InlC. Alternatively, blocking the interaction of N-WASP with Tuba SH3-6 would remove N-WASP from the equation, indicating whether other physiological partners of Tuba SH3-6 exist. Targeted residues including asparagine 1535, glutamate 1575,

tyrosine 1570 and tryptophan 1554 were successfully replaced with alanine to yield Tuba SH3-6 variants N1535A, E1575A, Y1570A and W1554A, respectively as shown in Figure 3.1.

4.2 Production and purification of Tuba SH3-6

Both wild-type and variants of Tuba SH3-6 were produced for biophysical and crystallography experiments. Similarly to Polle *et al.* (2014), variants of Tuba SH3-6 were produced efficiently as soluble protein by transforming *E. coli* BL21 strain with modified plasmid and growing the resulting culture in LB medium at 25 °C for 15 h after IPTG induction. *E. coli* is often used as the host in large scale recombinant protein production. This is due to its fast growth, simple nutrient requirements and well known genetics, which makes it easier to manipulate (Gopal and Kumar, 2013). Proteins were produced in pGEX-6P-1 vector with an N-terminal Glutathione S-transferase (GST) fused to the target protein. Produced proteins were purified by Glutathione Sepharose (GS) affinity chromatography. GST fusion tag is often used to produce highly soluble protein, because it can serve as a chaperone to ensure proper protein folding. However, this technique was used to capture the GST fusion protein by immobilized GS beads, since GST has high affinity for reduced glutathione (Einarson *et al.*, 2007, Harper and Speicher, 2011). The unbound proteins were washed out with 1 x PBS. To eliminate GST affecting other downstream experiments, it was separated from the target protein. This was achieved by HRV-3C protease cleavage between Gln and Gly residues of GST C-terminal sequence (Leu-Phe-Gln-Gly-Pro) (Harper and Speicher, 2011). After HRV-3C cleavage, the GST was left bound to the GS beads and the target protein was eluted with 1 x PBS (pH 7.4). However, the target protein eluted with some GST, suggesting that possibly there was leakage of GS beads during the coupling of protein extracts with the GS beads. This leakage was observed by SDS-PAGE (Figure 3.3) after GS affinity chromatography, hence the target protein was further purified using size exclusion chromatography (Figure 3.3). This was also the second line of purification used by Polle *et al.* (2014) to purify Tuba proteins.

Size exclusion chromatography is a useful method, permitting biomolecules of different molecular weights to be separated. Thus, when a sample is applied to a column the larger molecule elutes first, whilst the smaller molecules elute later because they enter the column pores (Campbell and Farrell, 2011). In this study, the strategy was to use ENrich SEC 70 10/300

column, which separates biomolecules ranging from 500 to 70 000 Da. The large size difference between GST (~26 kDa) and Tuba SH3-6 (~7.5 kDa) made it possible to separate Tuba SH3-6 from GST. Two peaks were observed on the chromatogram. The first peak observed had an elution volume of around 9 mL, suggesting a GST protein of higher molecular weight than the target protein. The second peak had an elution volume of around 15 mL, similar to the target protein eluted by (Polle *et al.*, 2014). Sample purity was analysed by SDS-PAGE as shown in Figure 3.3. Final protein concentrations ranging from 10 to 30 mg/ml were obtained and stored at 4 °C.

4.3 Production and purification of InlC

His_6-InlC fusion protein was produced and subsequently purified by IMAC. It was produced efficiently in *E. coli* BL21 cells at 20 °C in LB medium for 18 h after IPTG induction. These conditions were critical to consider in InlC production as different conditions affected protein solubility. IMAC technique is dependent on histidine strongly interacting with transition metals such as Co^{2+}, Ni^{2+}, Cu^{2+} and Zn^{2+}, which forms part of the matrix (beads). In this study, soluble His_6-InlC fusion protein extract was added to chelating agarose beads charged with Ni^{2+} ions. After washing of the unbound proteins from the matrix, the target protein was eluted with elution buffer containing 200 mM imidazole (Bornhorst and Falke, 2000). Impurities present in eluted InlC samples from IMAC suggests that the washing of the unbound proteins was insufficient. Hence, thorough washing or further purification was necessary to remove enough unbound proteins to eliminate interference with other downstream experiments.

4.4 Biophysical characterisation by Isothermal titration calorimetry

Isothermal titration calorimetry (ITC) is a gold-standard technique exploited to characterise interaction of biomolecules in their native state (Doyle, 1997). ITC was used to determine the binding affinities between variants of Tuba SH3-6 and its binding partner (either InlC or N-WASP) when an amino acid in Tuba SH3-6 is replaced with alanine. Protein samples used in ITC experiments need to be pure, appropriately concentrated and critically need to be in the same buffer as mismatched buffers result in heat of dilution, which can mask the reaction being analysed. Buffers of proteins were therefore replaced by standard buffers by size exclusion

chromatography. Protein samples were kept in 1 x PBS pH 7.4 (Polle *et al.*, 2014) because binding only occurred at a pH of 7 but diminished above pH 8. This implies that the binding reaction is pH-dependent presumably due to the protonation possibly of a histidine near the interface (Leavitt and Freire, 2001). It was critical to ensure that the same buffer with right pH was used. Table 4.1 summarizes K_D values obtained in this study and by Polle *et al.*, 2014 in ITC experiments for variants of Tuba SH3-6 with either InlC or N-WASP.

Table 4.1: Summarized outcome of expected and experimental interaction for Tuba SH3-6 variants with either InlC or N-WASP

Tuba SH3-6 variants	**Expected outcome with InlC**	**Experimental outcome with InlC**	**Expected outcome with N-WASP**	**Experimental outcome with N-WASP**
Wild-type	K_D = 5.4 µM (Polle *et al.*, 2014)	K_D = 1.3 µM	K_D = 46.5 µM (Polle *et al.*, 2014)	Indeterminate (due to probable N-WASP dimerization)
N1535A	K_D = 1.3 µM, Interaction unaffected	K_D = 1.2 µM, Interaction unaffected	K_D > 46.5 µM, Weakened interaction	Indeterminate (due to probable N-WASP dimerization)
E1575A	K_D = 1.3 µM, Interaction unaffected	K_D = 3.1 µM, Weakened interaction	K_D > 46.5 µM, Weakened interaction	K_D = 1.6 µM, Interaction strengthened
Y1570A	K_D > 1.3 µM, Weakened interaction	Indeterminate (due to probable InlC dimerization)	K_D = 46.5 µM, Unaffected interaction	Indeterminate (due to probable N-WASP dimerization)
W1554A	K_D > 1.3 µM, Weakened interaction	Indeterminate (due to probable InlC dimerization)	K_D = 46.5 µM, Unaffected interaction	Indeterminate (due to probable N-WASP dimerization)

Control ITC experiments for wild-type proteins were tested to check instrument functionality, data reliability and to compare with previous ITC experiments by (Polle *et al.*, 2014). This also served as reference point for the other experiments that were conducted. The ITC result confirmed complex formation between wild-type Tuba SH3-6 and InlC. A sigmoidal curve, which is an indication of a binding reaction is observed in the bottom panel of Figure 3.6 (A) with a

decreased K_D value (1.3 µM) relative to a published K_D of 5.4 µM determined by Polle *et al.*, 2014. The elevated binding affinity is possibly due to a different model of ITC instrument being used. The difference was less than an order of magnitude and relative affinities comparable. Thus, the results were interpreted as generally consistent. The ITC result between wild-type Tuba SH3-6 and N-WASP, yielded no protein interaction but N-WASP dimers or oligomers separating into monomers. The apparent dissociation constant for this reaction was quantified as K_D = 25 µM.

Tuba SH3-6 variants N1535A and E1575A were designed to affect its binding of N-WASP (K_D > 46.5 µM), without any impact on InlC binding (K_D = 1.3 µM). When InlC was titrated into the variant N1535A, an interaction was observed with no significant change in the experimental K_D value (1.2 µM) relative to the control experiment with wild-type proteins (as planned). Titrating InlC into the variant E1575A yielded a weaker interaction, with an increased K_D value (3.1 µM) relative to the control experiment, indicating that, contrary to expectations, the modification of Tuba SH3-6 had slightly impacted the binding affinity. Titrating N-WASP into the variant N1535A yielded an unexpected exponential curve rather than a sigmoidal curve, indication of N-WASP dimer dissociation with an apparent K_D value (40 µM). No binding event was witnessed and the experiment was not compared to control experiment with wild-type proteins. However, titrating N-WASP into the variant E1575A yielded a step curve, which indicated interaction between the two proteins with high concentrations. The apparent dissociation constant for this molecular interaction had decreased K_D value (1.6 µM) relative to the control experiment, confirming a stronger binding.

Tuba SH3-6 variants Y1570A and W1554A were designed to interfere with binding of InlC (K_D > 1.3 µM), without any impact on N-WASP binding (K_D = 46.5 µM). InlC reaction with either Y1570A or W1554A yielded an unexpected exponential curve rather than a sigmoidal curve. The exponential curves were proposed to be due to dissociation of InlC dimers induced by concentrating InlC to the required level (ITC Tutorial Guide, MicroCal, Malvern, USA). Similarly, titrating N-WASP into either Y1570A or W1554A variant yielded dissociation of N-WASP dimers with apparent K_D of 89 µM and 35 µM, respectively. No binding event was witnessed and the experiments were not compared to control experiments with wild-type proteins. The heat of

the suggested InlC or N-WASP dimer dissolution is presumably significantly larger than the heat released from InlC or N-WASP binding to Tuba SH3-6 variant Y1570A, masking the latter. The suggested InlC or N-WASP dimer dissolution could potentially be confirmed by repeating the experiment without adding either Tuba SH3-6 Y1570A or W1554A, which should result in the same curve as seen before.

4.5 Crystallization

To understand how variant Tuba SH3-6 interacts with its partner (either InlC or N-WASP) on an atomic level, the aim was to co-crystallise the protein complexes. However, no protein complex crystal was obtained in this study. Instead a crystal structure of InlC was determined with improved resolution. InlC-only crystals were also reported when using wild-type InlC in co-crystallization experiments (Polle *et al.*, 2014). This was proposed to be due to InlC crystal packing involving aromatic residues found at the Ig-like domain (Ooi *et al.*, 2006). Hence, Tyr246 and Tyr247 at this domain were substituted by alanine residues to yield Tuba SH3-6 / InlC complex crystals (Polle *et al.*, 2014).

Here, an oval-shaped crystal (Figure 3.11) with a longest axis of 755 µm was obtained from a reservoir solution consisting of 3 M NaCl, and 1 M Bis-Tris pH 6.5. This crystallization condition was different to that of Ooi *et al.*, 2006: 1.8 M $MgSO_4$, and 0.1 M MES pH 6.5. The condition thus varied with respect to the salt and the precipitant used for crystallization. Nevertheless, both crystals shared the same orthorhombic space group of $P2_12_12$.

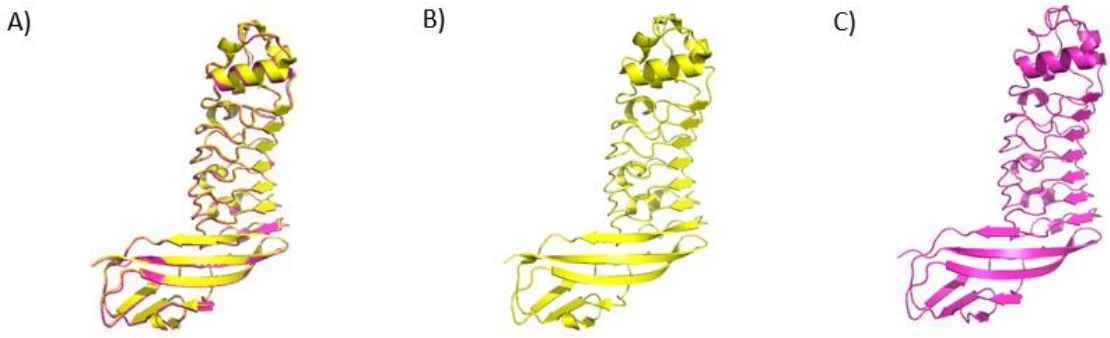

Figure 4.1: **Comparison of solved InlC structure with homolog.**
A) Homolog structure superimposed onto solved InlC structure. B) The homolog structure (yellow) reported by Ooi *et al.*, 2006. C) The solved InlC structure (purple).

To compare the solved InlC structure with the homolog structure reported by Ooi *et al.*, 2006, it was super-positioned onto the homolog (PDB code: 1XEU)) using PyMol (DeLano, 2002) (Figure 4.1 A). The superposition reveals a high degree of similarity between the solved InlC and the homolog by Ooi *et al.*, 2006. No conformational change was visible between the superimposed structures.

5 Conclusion

Variants of Tuba SH3-6 and wild-type InlC were successfully produced and purified. Downstream experiments with ITC were used to determine the binding affinities between variant of Tuba SH3-6 variants and its binding partners (InlC or N-WASP). Overall, only variant E1575A had an impact on interaction with its binding partner. The variant E1575A yielded a weaker and stronger interaction with InlC and N-WASP, respectively. This variant will be useful in an *in vivo study* to further investigate the underlying factors involved in cell-to-cell spread. The experiment to investigate InlC or N-WASP interaction with either N1535A, Y1570A or W1554A would need to be redesigned to prevent InlC or N-WASP dimerization. For future work, different and multiple amino acid substitutions could be exploited to enhance effect on binding interaction. By doing so, it will provide a better molecular tool to further investigate the underlying factors involved in cell-to-cell spread in *in vivo* study.

While no protein complex crystal was obtained, InlC-only crystal structure was determined with an improved resolution at 1.85 Å relative to 2.05 Å deposited onto the protein data base (PDB code: 1XEU). The newly solved InlC structure will be deposited onto PDB. For future work, co-crystallization experiments will have InlC variant with Tyr246 and Tyr247 replaced with alanine to prevent InlC-only crystal.

References

1. ALBERTS, B., JOHNSON, A., LEWIS, J., RAFF, M., ROBERTS, K. & WALTER, P. 2002. Molecular Biology of the Cell 4th edn (New York: Garland Science). *Annals of Botany,* 91**,** 401.
2. ALLERBERGER, F. & WAGNER, M. 2010. Listeriosis: a resurgent foodborne infection. *Clinical Microbiology and Infection,* 16**,** 16-23.
3. AURELI, P., FIORUCCI, G. C., CAROLI, D., MARCHIARO, G., NOVARA, O., LEONE, L. & SALMASO, S. 2000. An outbreak of febrile gastroenteritis associated with corn contaminated by *Listeria monocytogenes*. *New England Journal of Medicine,* 342**,** 1236-1241.
4. BARBUDDHE, S. B. & CHAKRABORTY, T. 2009. Listeria as an enteroinvasive gastrointestinal pathogen. *Current Topics in Microbiology and Immunology,* 337**,** 173-95.
5. BIERNE, H. & COSSART, P. 2007. *Listeria monocytogenes* surface proteins: from genome predictions to function. *Microbiology and Molecular Biology Review.,* 71**,** 377-397.
6. BIERNE, H., MAZMANIAN, S. K., TROST, M., PUCCIARELLI, M. G., LIU, G., DEHOUX, P., CONSORTIUM, E. L. G., JÄNSCH, L., PORTILLO, F. G. D. & SCHNEEWIND, O. 2002. Inactivation of the srtA gene in *Listeria monocytogenes* inhibits anchoring of surface proteins and affects virulence. *Molecular Microbiology,* 43**,** 869-881.
7. BOLANOS-GARCIA, V. M. & CHAYEN, N. E. 2009. New directions in conventional methods of protein crystallization. *Progress in Biophysics and Molecular biology,* 101**,** 3-12.
8. BORNHORST, J. A. & FALKE, J. J. 2000. [16] Purification of proteins using polyhistidine affinity tags. *Methods in Enzymology.* Elsevier.
9. BUCHRIESER, C. 2007. Biodiversity of the species *Listeria monocytogenes* and the genus Listeria. *Microbes and Infection,* 9**,** 1147-1155.
10. CABANES, D., DEHOUX, P., DUSSURGET, O., FRANGEUL, L. & COSSART, P. 2002. Surface proteins and the pathogenic potential of *Listeria monocytogenes*. *Trends in Microbiology,* 10**,** 238-245.
11. CAMEJO, A., CARVALHO, F., REIS, O., LEITÃO, E., SOUSA, S. & CABANES, D. 2011. The arsenal of virulence factors deployed by *Listeria monocytogenes* to promote its cell infection cycle. *Virulence,* 2**,** 379-394.
12. CAMPBELL, M. & FARRELL, S. 2011. Biochemistry, Cengage Learning. Boston.
13. CHAYEN, N. E. & SARIDAKIS, E. 2008. Protein crystallization: from purified protein to diffraction-quality crystal. *Nature Methods,* 5**,** 147.
14. COSSART, P. & SANSONETTI, P. J. 2004. Bacterial Invasion: The Paradigms of Enteroinvasive Pathogens. *Science,* 304**,** 242-248.
15. COSSART, P. & TOLEDO-ARANA, A. 2008. *Listeria monocytogenes*, a unique model in infection biology: an overview. *Microbes and Infection,* 10**,** 1041-1050.
16. DEAN, S. J. & FARMER, M. 2017. Pediatric cancer genetics. *Current Opinion in Pediatrics,* 29**,** 629-633.
17. DELANO, W. L. 2002. The PyMOL Molecular Graphics System (Scientific, D., ed) Schrödinger. *LLC, New York*.
18. DESSAU, M. A. & MODIS, Y. 2011. Protein crystallization for X-ray crystallography. *JoVE (Journal of Visualized Experiments)***,** e2285.
19. DORAN, K. S., BANERJEE, A., DISSON, O. & LECUIT, M. 2013. Concepts and mechanisms: crossing host barriers. *Cold Spring Harbor Perspectives in Medicine,* 3**,** a010090.
20. DOWER, W. J., MILLER, J. F. & RAGSDALE, C. W. 1988. High efficiency transformation of E. coli by high voltage electroporation. *Nucleic Acids Research,* 16**,** 6127-6145.

21. DOYLE, M. L. 1997. Characterization of binding interactions by isothermal titration calorimetry. *Current Opinion in Biotechnology,* 8**,** 31-35.
22. EINARSON, M. B., PUGACHEVA, E. N. & ORLINICK, J. R. 2007. Preparation of GST fusion proteins. *Cold Spring Harbor Protocols,* 2007**,** pdb. prot4738.
23. EMSLEY, P. & COWTAN, K. 2004. Coot: model-building tools for molecular graphics. *Acta Crystallographica Section D: Biological Crystallography,* 60**,** 2126-2132.
24. ENGELBRECHT, F., CHUN, S. K., OCHS, C., HESS, J., LOTTSPEICH, F., GOEBEL, W. & SOKOLOVIC, Z. 1996. A new PrfA-regulated gene of *Listeria monocytogenes* encoding a small, secreted protein which belongs to the family of internalins. *Molecular Microbiology,* 21**,** 823-837.
25. FURRER, B., CANDRIAN, U., HOEFELEIN, C. & LUETHY, J. 1991. Detection and identification of *Listeria monocytogenes* in cooked sausage products and in milk by in vitro amplification of haemolysin gene fragments. *Journal of Applied Bacteriology,* 70**,** 372-379.
26. GOPAL, G. J. & KUMAR, A. 2013. Strategies for the production of recombinant protein in Escherichia coli. *The protein journal,* 32**,** 419-425.
27. GOULET, V., HEBERT, M., HEDBERG, C., LAURENT, E., VAILLANT, V., DE VALK, H. & DESENCLOS, J.-C. 2011. Incidence of listeriosis and related mortality among groups at risk of acquiring listeriosis. *Clinical Infectious Diseases,* 54**,** 652-660.
28. GOULET, V., KING, L. A., VAILLANT, V. & DE VALK, H. 2013. What is the incubation period for listeriosis? *BMC Infectious Diseases,* 13**,** 11.
29. GRAVES, L. M., HELSEL, L. O., STEIGERWALT, A. G., MOREY, R. E., DANESHVAR, M. I., ROOF, S. E., ORSI, R. H., FORTES, E. D., MILILLO, S. R. & DEN BAKKER, H. C. 2010. Listeria marthii sp. nov., isolated from the natural environment, Finger Lakes National Forest. *International Journal of Systematic and evolutionary microbiology,* 60**,** 1280-1288.
30. GRAY, M. L. & KILLINGER, A. 1966. *Listeria monocytogenes* and listeric infections. *Bacteriological reviews,* 30**,** 309.
31. GREEN, R. & ROGERS, E. J. 2013. Chemical transformation of E. coli. *Methods in enzymology,* 529**,** 329.
32. HARPER, S. & SPEICHER, D. W. 2011. Purification of proteins fused to glutathione S-transferase. *Protein Chromatography.* Springer.
33. HE, F. 2011. Laemmli-sds-page. *Bio-protocolBio101: e80*.
34. HOF, H. 2003. History and epidemiology of listeriosis. *FEMS Immunology & Medical Microbiology,* 35**,** 199-202.
35. HOLLAND, E. G., ACCA, F. E., BELANGER, K. M., BYLO, M. E., KAY, B. K., WEINER, M. P. & KISS, M. M. 2015. In vivo elimination of parental clones in general and site-directed mutagenesis. *Journal of Immunological Methods,* 417**,** 67-75.
36. IRETON, K. 2013. Molecular mechanisms of cell–cell spread of intracellular bacterial pathogens. *Open Biology,* 3**,** 130079.
37. JACOBS, T., DARJI, A., FRAHM, N., ROHDE, M., WEHLAND, J., CHAKRABORTY, T. & WEISS, S. 1998. Listeriolysin O: cholesterol inhibits cytolysis but not binding to cellular membranes. *Molecular Microbiology,* 28**,** 1081-1089.
38. KOCKS, C., GOUIN, E., TABOURET, M., BERCHE, P., OHAYON, H. & COSSART, P. 1992. *L. monocytogenes*-induced actin assembly requires the actA gene product, a surface protein. *Cell,* 68**,** 521-531.
39. KOVACS, E. M., MAKAR, R. S. & GERTLER, F. B. 2006. Tuba stimulates intracellular N-WASP-dependent actin assembly. *Journal of Cell Science,* 119**,** 2715-2726.
40. KUCHENMÜLLER, T., ABELA-RIDDER, B., CORRIGAN, T. & TRITSCHER, A. 2013. World Health Organization Initiative to Estimate the Global Burden of Foodborne Diseases. *Scientific and Technical Review of the Office International des Epizooties,* 32**,** 459-467.

41. LEAVITT, S. & FREIRE, E. 2001. Direct measurement of protein binding energetics by isothermal titration calorimetry. *Current Opinion in Structural Biology,* 11**,** 560-566.
42. LECUIT, M. 2005. Understanding how *Listeria monocytogenes* targets and crosses host barriers. *Clinical Microbiology and Infection,* 11**,** 430-436.
43. LECUIT, M. 2007. Human listeriosis and animal models. *Microbes and Infection,* 9**,** 1216-1225.
44. LECUIT, M., OHAYON, H., BRAUN, L., MENGAUD, J. & COSSART, P. 1997. Internalin of *Listeria monocytogenes* with an intact leucine-rich repeat region is sufficient to promote internalization. *Infection and Immunity,* 65**,** 5309-5319.
45. LEUNG, N., GIANFELICE, A., GRAY-OWEN, S. D. & IRETON, K. 2013. Impact of the *Listeria monocytogenes* protein InlC on infection in mice. *Infection and Immunity,* 81**,** 1334-1340.
46. LIU, H. & NAISMITH, J. H. 2008. An efficient one-step site-directed deletion, insertion, single and multiple-site plasmid mutagenesis protocol. *BMC Biotechnology,* 8**,** 91.
47. LODISH, H., BERK, A., ZIPURSKY, S. L., MATSUDAIRA, P., BALTIMORE, D. & DARNELL, J. 2000. DNA cloning with plasmid vectors. *Molecular Cell Biology. 4th edition.* WH Freeman.
48. LU, L., PATEL, H. & BISSLER, J. J. 2002. Optimizing Dpn I Digestion Conditions to Detect Replicated DNA. *Biotechniques,* 33**,** 316-318.
49. MCCOY, A. J., GROSSE-KUNSTLEVE, R. W., ADAMS, P. D., WINN, M. D., STORONI, L. C. & READ, R. J. 2007. Phaser crystallographic software. *Journal of Applied Crystallography,* 40**,** 658-674.
50. MENGAUD, J., OHAYON, H., GOUNON, P., MÈGE, R.-M. & COSSART, P. 1996. E-cadherin is the receptor for internalin, a surface protein required for entry of *L. monocytogenes* into epithelial cells. *Cell,* 84**,** 923-932.
51. MENGAUD, J., VICENTE, M., CHENEVERT, J., PEREIRA, J. M., GEOFFROY, C., GICQUEL-SANZEY, B., BAQUERO, F., PEREZ-DIAZ, J. & COSSART, P. 1988. Expression in Escherichia coli and sequence analysis of the listeriolysin O determinant of *Listeria monocytogenes*. *Infection and Immunity,* 56**,** 766-772.
52. NEWELL, D. G., KOOPMANS, M., VERHOEF, L., DUIZER, E., AIDARA-KANE, A., SPRONG, H., OPSTEEGH, M., LANGELAAR, M., THREFALL, J. & SCHEUTZ, F. 2010. Food-borne diseases—the challenges of 20 years ago still persist while new ones continue to emerge. *International Journal of Food Microbiology,* 139**,** S3-S15.
53. NIKITAS, G., DESCHAMPS, C., DISSON, O., NIAULT, T., COSSART, P. & LECUIT, M. 2011. Transcytosis of *Listeria monocytogenes* across the intestinal barrier upon specific targeting of goblet cell accessible E-cadherin. *Journal of Experimental Medicine,* 208**,** 2263-2277.
54. OOI, A., HUSSAIN, S., SEYEDARABI, A. & PICKERSGILL, R. W. 2006. Structure of internalin C from *Listeria monocytogenes*. *Acta Crystallographica Section D: Biological Crystallography,* 62**,** 1287-1293.
55. ORSI, R. H., DEN BAKKER, H. C. & WIEDMANN, M. 2011. *Listeria monocytogenes* lineages: genomics, evolution, ecology, and phenotypic characteristics. *International Journal of Medical Microbiology,* 301**,** 79-96.
56. OTANI, T., ICHII, T., AONO, S. & TAKEICHI, M. 2006. Cdc42 GEF Tuba regulates the junctional configuration of simple epithelial cells. *The Journal of Cell Biology,* 175**,** 135-146.
57. PAMER, E. G. 2004. Immune responses to *Listeria monocytogenes*. *Nature Reviews Immunology,* 4**,** 812-823.
58. PIZARRO-CERDÁ, J. & COSSART, P. 2006. Subversion of cellular functions by *Listeria monocytogenes*. *The Journal of Pathology: A Journal of the Pathological Society of Great Britain and Ireland,* 208**,** 215-223.
59. POLLE, L., RIGANO, L. A., JULIAN, R., IRETON, K. & SCHUBERT, W.-D. 2014. Structural details of human Tuba recruitment by InlC of *Listeria monocytogenes* elucidate bacterial cell-cell spreading. *Structure,* 22**,** 304-314.

60. PÖNTINEN, A., MARKKULA, A., LINDSTRÖM, M. & KORKEALA, H. 2015. Two-component-system histidine kinases involved in growth of *Listeria monocytogenes* EGD-e at low temperatures. *Applied and Environment Microbiology,* 81**,** 3994-4004.
61. RAJABIAN, T., GAVICHERLA, B., HEISIG, M., MÜLLER-ALTROCK, S., GOEBEL, W., GRAY-OWEN, S. D. & IRETON, K. 2009. The bacterial virulence factor InlC perturbs apical cell junctions and promotes cell-to-cell spread of Listeria. *Nature Cell Biology,* 11**,** 1212.
62. REIS, R. S. & HORN, F. 2010. Enteropathogenic Escherichia coli, Samonella, Shigella and Yersinia: cellular aspects of host-bacteria interactions in enteric diseases. *Gut Pathogens,* 2**,** 1757-4749.
63. SALAZAR, M. A., KWIATKOWSKI, A. V., PELLEGRINI, L., CESTRA, G., BUTLER, M. H., ROSSMAN, K. L., SERNA, D. M., SONDEK, J., GERTLER, F. B. & DE CAMILLI, P. 2003. Tuba, a novel protein containing bin/amphiphysin/Rvs and Dbl homology domains, links dynamin to regulation of the actin cytoskeleton. *Journal of Biological Chemistry,* 278**,** 49031-49043.
64. SAMBROOK, J. & RUSSELL, D. 2001. Molecular cloning: A laboratory manual, the third edition. Cold spring harbor laboratory press, cold spring harbor, New York.
65. SCHLECH III, W. F. & ACHESON, D. 2000. Foodborne listeriosis. *Clinical Infectious Diseases,* 31**,** 770-775.
66. SCHNUPF, P. & PORTNOY, D. A. 2007. Listeriolysin O: a phagosome-specific lysin. *Microbes and Infection,* 9**,** 1176-1187.
67. SCHUBERT, W.-D., GÖBEL, G., DIEPHOLZ, M., DARJI, A., KLOER, D., HAIN, T., CHAKRABORTY, T., WEHLAND, J., DOMANN, E. & HEINZ, D. W. 2001. Internalins from the human pathogen *Listeria monocytogenes* combine three distinct folds into a contiguous internalin domain. *Journal of Molecular Biology,* 312**,** 783-794.
68. SMITH, G. A., MARQUIS, H., JONES, S., JOHNSTON, N. C., PORTNOY, D. A. & GOLDFINE, H. 1995. The two distinct phospholipases C of *Listeria monocytogenes* have overlapping roles in escape from a vacuole and cell-to-cell spread. *Infection and Immunity,* 63**,** 4231-4237.
69. TOUNGE, B. A. & PARKER, M. H. 2011. Designing a diverse high-quality library for crystallography-based FBDD screening. *Methods in enzymology.* Elsevier.
70. TRAVIER, L., GUADAGNINI, S., GOUIN, E., DUFOUR, A., CHENAL-FRANCISQUE, V., COSSART, P., OLIVO-MARIN, J.-C., GHIGO, J.-M., DISSON, O. & LECUIT, M. 2013. ActA promotes *Listeria monocytogenes* aggregation, intestinal colonization and carriage. *PLoS Pathogens,* 9**,** e1003131.
71. VÁZQUEZ-BOLAND, J. A., KUHN, M., BERCHE, P., CHAKRABORTY, T., DOMíNGUEZ-BERNAL, G., GOEBEL, W., GONZÁLEZ-ZORN, B., WEHLAND, J. & KREFT, J. 2001. Listeria pathogenesis and molecular virulence determinants. *Clinical Microbiology Reviews,* 14**,** 584-640.
72. WELCH, M. D., ROSENBLATT, J., SKOBLE, J., PORTNOY, D. A. & MITCHISON, T. J. 1998. Interaction of human Arp2/3 complex and the *Listeria monocytogenes* ActA protein in actin filament nucleation. *Science,* 281**,** 105-108.
73. WHO 2018. Listeriosis–South Africa. *Disease outbreak news. http://www. who. int/csr/don/28-march-2018-listeriosis-south-africa/en/. Accessed,* 2.